

Extended abstract J8 . 3

Third Symposium on Aerosol-Cloud-Climate Interactions, The AMS 91st
Annual Meeting, 23-27 January 2011 in Seattle, WA.

The role of small soluble aerosols in the microphysics of deep maritime clouds

A. P. Khain (1), V. Phillips (2), N. Benmoshe (1) and A. Pokrovsky (1)

(1) Department of Atmospheric Sciences, The Hebrew University of Jerusalem, Israel

(2) The Department of Meteorology, University of Hawaii at Manoa, Honolulu, USA

Communicating author: Prof. Alexander Khain, Department of Atmospheric sciences, The Hebrew University of Jerusalem, Jerusalem, Givat Ram, 91904, email: khain@vms.huji.ac.il

Abstract

Some observational evidence such as bi-modal size distributions, comparatively high concentrations of supercooled drops at upper levels, high concentrations of small ice crystals in cloud anvils leading to high optical depth, as well as lightning that can take place in the eye walls of hurricanes, indicate that the traditional view to microphysics of deep maritime clouds requires, possibly, some revisions.

Numerical simulations using the spectral microphysics Hebrew University cloud model show that these observed features can be attributed to existence in the atmosphere of small aerosols with diameters less than about $0.05 \mu m$ in the cloud condensational nuclei (CCN) size spectra. Intense drop collisions below and around the freezing level lead to a dramatic decrease in droplet concentration during ascent in convective updrafts. Being accompanied by intense vertical

velocity, this decrease in the drop concentration leads to a dramatic increase in supersaturation, activation of the smallest CCN aerosols and production of new droplets several kilometers above cloud base. The increase in supersaturation and in-cloud nucleation during ascent can also be partly related to a decrease in droplet concentration by riming at cold temperatures. Successive growth of these droplets leads to formation of supercooled water and significant ice crystal concentrations aloft. The role of giant CCN is reconsidered. The synergetic effect of the smallest CCN and giant CCN in production of small supercooled water and ice crystals in cloud anvils is analyzed. Significant effects from small aerosols on various microphysical parameters of clouds such as precipitation, cloud updrafts and radar reflectivity were found. The possible role of these small aerosols in formation of conditions favorable for lightning in deep maritime clouds is discussed. As far as we are aware, this is the first study in the literature to chart the diverse impacts, on the physics and dynamics of maritime deep convection, from such soluble aerosols smaller than $0.05 \mu m$.

1. Introduction

There are several thermodynamical and microphysical features that typify deep convective maritime clouds in the Tropics: a) these clouds develop in a humid atmosphere, so the cloud base is located between 1 and 2 km altitude; b) the freezing level is quite high (4-4.5 km); c) The concentration of cloud condensational nuclei (CCN) (at 1% supersaturation S_w) is about 60-200 cm^{-3} (Pruppacher and Klett 1997; Levin and Cotton 2009), which is about an order of magnitude lower than that for clouds developing over continents; d) it is widely accepted that aerosol size distributions over the sea (especially at strong wind conditions) contain high concentrations of giant CCN (hereafter GCCN) with dry radii exceeding $1 \mu m$ especially under strong wind conditions because of their production by sea spray.

Low CCN concentrations and the existence of GCCN determine typical maritime properties of these clouds, characterized by low droplet concentrations of about 50-150 cm^{-3} , and rapid formation of raindrops below the level of 4-5 km altitude. The raindrops, in turn, collect most of the drops nucleated near the cloud base, leading to intense warm rain. Comparatively rare drops that did not fall out below 4-5 km level, freeze within the layer between 5 and 6 km altitude, forming frozen drops (or graupel) of a comparatively low concentration (e.g., Blyth et al. 1998;

Yin et al , 2000; Ovtchinnikov et al, 2000; Rosenfeld et al 2002; Khain et al. 2004; Phillips et al. 2005; Takahashi, 2006; Freud et al 2008).

It is widely accepted that these clouds should not have any significant supercooled cloud-liquid at high altitudes (~8-10 km) or any significant concentration of ice crystals (see reviews by Rosenfeld et al, 2008; Khain 2009). According to this view drop concentrations at levels of homogeneous freezing (~9.5-10 km) should be negligible, so that these clouds should contain very low concentrations of ice crystals in anvils of deep convective clouds and related cirrus clouds.

For instance, one of the important concepts of the STORMFURY (1965-1975) project (according to which the weakening of TC was supposed to reach by glaciogenic seeding with AgI of cloud anvils at the eye wall periphery) was the assumption that there is only a little natural ice crystals in the cloud anvils (Willoughby et al. 1985).

Contrary to this view of the microphysics of maritime clouds, there are *indirect and direct* evidences of the existence of small supercooled droplets at the upper levels of deep tropical clouds which can be the source of high ice crystal concentration in the cloud anvils. To the *indirect evidence* one can attribute the existence of lightning in tropical cyclone (TC) eyewalls and maritime deep convection in the InterTropical Convergence Zone (ITCZ). According to a widely accepted concept, the charge separation in clouds takes place at sub-zero temperatures (about -20°C and colder), where collisions between low and high density ice particles take place in the presence of a significant amount of supercooled liquid water (e.g., Black and Hallet 1999; Saunders 1993, Cecil et al 2002a,b; Sherwood et al 2006; Takahashi 1978, 1984; Jayaratne *et al.* 1983; Baker *et al.* 1987; Kumar and Saunders 1989; Saunders *et al.* 1991). The significant difference in lightning density over the land and the sea is well known (e.g., Christian et al. 2003; Williams and Satori, 2004; Williams et al. 2004; Sherwood et al. 2006). The lower frequency of lightning over the sea is usually attributed to weaker vertical velocities in maritime convection and to low aerosol concentrations. Both factors also favor the formation of raindrops below freezing level collecting most of the droplets nucleated near the cloud base. It is assumed that this effect should dramatically decrease the amount of supercooled water droplets aloft, inhibiting the charge separation process. One could expect that such a decrease in the amount of supercooled water aloft should be especially strong in eyewalls of TCs, where a huge amount of GCCN is produced by spray leading to the dramatic intensification of warm rain (in this sense clouds in eyewall of TC can be referred to as extremely maritime).

Yet, contrary to what might be expected, satellite observations show intense lightning in clouds within the TC eyewall at the stage of a mature TC. If the concept of lightning formation is correct, such observations imply that supercooled droplets exist at upper levels even in extremely maritime clouds of a TC eyewall in the presence of dramatically high concentrations of GCCN caused by spray formation in zones of strong winds and extremely low concentration of CCN (measured at 1% of S_w). Hence, the question arises: "If warm rain processes in maritime clouds are so efficient, why do supercooled droplets and high concentrations of graupel and ice crystals exist so high aloft in maritime clouds with moderate updrafts to allow lightning formation in deep maritime convective clouds in the ITCZ and in the hurricane eyewalls?"

Evidence for a significant concentration of supercooled droplets at the upper levels of deep convective maritime clouds is provided by aircraft observations of supercooled water of $\sim 0.3 \text{ gm}^{-3}$ over the sea near Florida in deep convective updrafts with peak vertical velocities of up to about 20 m/s (Fridlind *et al.* 2004; Heymsfield *et al.* 2005; Phillips *et al.* 2005). These observations were part of an experiment referred to as: The Cirrus Regional Study of Tropical Anvils and Cirrus Layers - Florida Area Cirrus Experiment (CRYSTAL-FACE). Aircraft observations in the Kwajalein Experiment (KWAJEX) showed droplet concentrations of about 50 cm^{-3} up to 9 km altitude (about -30°C) throughout most of the depth of the mixed-phase region, averaged over deep, highly visible cloud-decks (Phillips *et al.* 2007a).

At last, detailed analysis of aircraft observations from 6 field experiments by Heymsfield *et al.* (2009) shows the existence of a significant concentrations of small supercooled droplets above ~ 6 km in maritime deep convective clouds. Note that the supercooled droplets existing at temperatures colder than about -20°C inevitably should be small, because rain drops almost immediately freeze at such low temperatures, partly by activation of their immersed ice nuclei or by collisions with crystals and other ice particles (Pruppacher and Klett 1997). Indeed, Heymsfield *et al.* (2009) reported that the size of these droplets aloft is typically below $50 \mu\text{m}$. In agreement with a significant concentration of small supercooled droplets at the upper levels of deep convective maritime clouds, Heymsfield *et al.* (2009) reported the concentration of ice crystals in anvils of strong deep maritime convective clouds at temperatures of -40°C as high as 30 cm^{-3} in relatively clean air, and 300 cm^{-3} in polluted clouds sampled off the west coast of Africa where the loading of Saharan dust is high. Such concentrations of ice crystals exceed the possible

concentration of active ice nuclei (IN) by several orders of magnitude, and can be attributed to *homogeneous freezing of cloud-droplets at temperatures as cold as -38 °C* (Rosenfeld and Woodley, 2000; Khain *et al.* 2001; Phillips *et al.* 2005, 2007a; Heymsfield *et al.* 2009).

It is interesting that according to Heymsfield *et al.* (2009) the mass content and concentration of supercooled droplets decrease in maritime clouds with height above the freezing level and actually disappear at temperatures of about -15 to -20 °C and then supercooled droplets arise at colder temperatures with their concentration increasing upward.

One can propose two mechanisms of formation of small supercooled droplets at temperatures colder than -15 °C or -20 °C. The first mechanism is in-cloud nucleation of unactivated CCN (following to Pruppacher and Klett [1997], we use here the terms "activated" and "non-activated" CCN, sum of which represents the concentration of condensation nuclei, CN) aerosols entrained laterally from the free troposphere into deep convective updrafts (Phillips *et al.* 2005; Fridlind *et al.* 2004; Yin *et al.* 2005). Entrainment allows it to occur even when vertical velocities are weak in clouds. For the vigorous thunderstorm case from Florida simulated by Phillips *et al.* (2005) and Fridlind *et al.* (2004) entrainment of aerosol particles (AP) aloft was found to be very efficient in production of small droplets.

In many cases, the concentration of CCN decreases with height exponentially (Levin and Cotton 2009). Here, the mechanism of the CCN entrainment through the lateral cloud boundaries at high levels is less efficient (as, for instance, in the hurricane eyewalls). In such cases, formation of small droplets can be attributed to in-cloud activation of CCN ascending from cloud base together with growing droplets. In-cloud nucleation in stratocumulus and cumulus clouds was found and discussed in some previous studies (e.g., Ochs 1978; Ludlam 1980; Song and Marwitz 1989; Korolev 1994; Pinsky and Khain 2002; Segal *et al.*, 2003; Phillips *et al.* 2005). For instance, Phillips *et al.* (2005) simulated, with a spectral (bin) microphysics model, a vigorous deep convective cell observed over the sea near Florida and found that the vast majority (99%) of supercooled cloud-droplets upwelled to the top of the mixed-phase region had been activated in-cloud ("secondary droplet nucleation"), far above cloud-base. They froze homogeneously near -36 °C, accounting for almost all of the cell's ice crystals at anvil levels.

The conceptual picture of such process is illustrated in **Figure 2** (Pinsky and Khain 2002 with changes). Let us assume that near cloud base the size distribution of aerosols (non-activated CCN) is wide and includes particles with dry radii ranged from 0.001 μm to $\sim 2 \mu\text{m}$ (Hobbs,

1993; Pruppacher and Klett 1997). The first CCN activation takes place within the supersaturation maximum located within a few tens of meters above cloud base (Rogers and Yau, 1989). The supersaturation maximum near the cloud base depends on vertical velocity at this level, which does not exceed a few m/s in maritime clouds (e.g. Heymsfield et al 2009). As a result, *only some fraction* of all CCN is activated at the cloud base. This statement was supported by detailed calculations of the droplet concentration at cloud base under different aerosol conditions and vertical velocities at cloud base performed by Segal and Khain (2006) and by comparison of their results with observations (e.g. Ramanathan et al, 2001; Martin et al 1994). The droplets formed near the cloud base give rise to the formation of the first mode in droplet size distribution (hereafter, DSD) (see **Figure 1**).

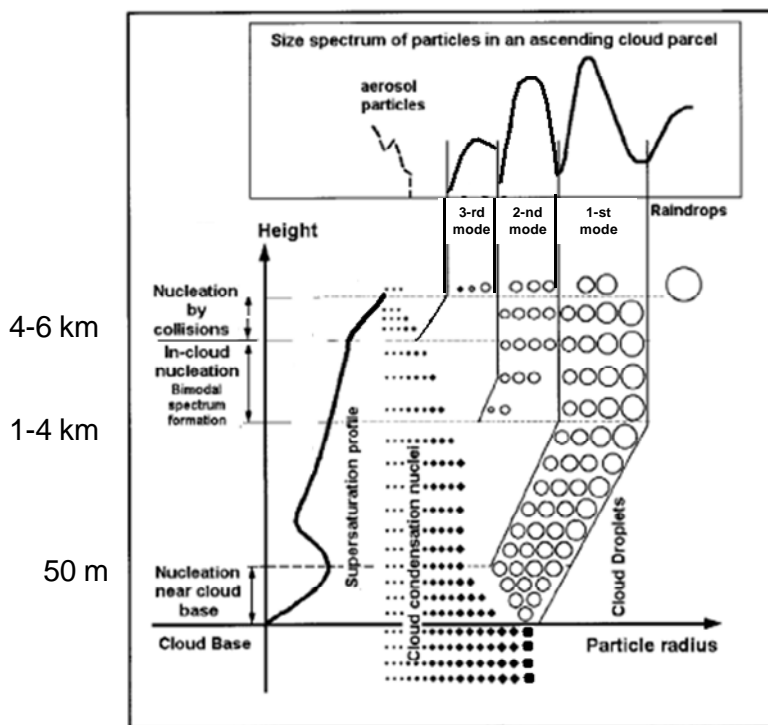


Figure 1. The conceptual scheme of droplet spectra formation in deep convective clouds (after Pinsky and Khain 2002 with changes). See text for details.

These droplets play a dominant role in the warm rain formation. Above the local supersaturation maximum near cloud base, S_w decreases with height, but then begins growing again during in-cloud ascent due to an increase with height of the vertical velocity. In case the S_w in updraft exceeds the local maximum reached earlier near the cloud base, new CCN activation (i.e., in-cloud nucleation of droplets) takes place giving rise to formation of the second cloud mode of the DSD. Typically the second mode (i.e., bi-modal DSD) forms a few hundred meters to

a few km above cloud base (as it was observed by Warner [1969a,b] and simulated by Pinsky and Khain [2002]; Segal et al [2003]). Note that in zones of efficient collisions between drop and rapid rain fallout, the droplet concentration decreases and vertical velocity increases (partially due to unloading of the large drops). As a result the S_w may dramatically increase and a new portion of the smallest CCN may be activated producing small droplets at heights of ~6 km above the cloud base. The thermodynamic and aerosol conditions leading to the formation of the bi-modal DSD were analyzed using a spectral bin microphysics (SBM) Lagrangian parcel model in which size distributions of aerosols and droplets were calculated on a movable mass grid containing 2000 mass bins (Pinsky and Khain 2002; Segal *et al* 2003). Note that the process of in-cloud nucleation of droplets takes place often at high supersaturations, so that nucleation of the smallest droplets is accompanied by their fast growth. As a result, the gaps between modes may disappear leading to a uni-modal DSD having a relative dispersion of 0.2-0.3 and containing smallest droplets at high levels aloft. Indeed, in-cloud activation of droplets may occur continuously over a deep layer of the cloudy updraft in which the vertical velocity increases with height, causing a steady increase with height of the in-cloud supersaturation.

In the present study, we argue that all phenomena mentioned above (formation of small supercooled droplets at temperatures colder than $-20\text{ }^{\circ}\text{C}$, formation of high concentration of ice crystals in anvils of deep convective clouds, lightning in extremely maritime clouds in the hurricane eyewall) may be caused by one and the same mechanism of in-cloud droplet nucleation, when the supersaturation S_w in ascending cloud parcels exceeds the values experienced by the parcels earlier. Such a rise in S_w can be caused by an increase in the vertical velocity above cloud base and the depletion of cloud-droplets by coalescence during deep maritime ascent (Ochs 1978; Pinsky and Khain 2002; Phillips et al. 2005). Pinsky and Khain (2002) showed that the combined effects of vertical velocity increase and the depletion of cloud droplets by coalescence can lead to formation of DSDs containing three modes.

Note that the hypothesis of in-cloud nucleation in air ascending from the cloud base requires the existence of very small CCN with diameters smaller than about $0.03\ \mu\text{m}$, which can be activated only at high S_w exceeding 1%. These CCN cannot be activated at the cloud base of maritime clouds, where S_w has a peak of about 0.1-1%. Besides, these CCN can scarcely be scavenged by precipitation because of their small sizes and very low collision efficiencies, with

very low rates of scavenging (Flossmann and Pruppacher 1987). As a result, both droplets and haze particles (not activated CCN) ascend within updrafts above cloud base.

So, the explanation of the phenomena listed above reduces to answering the following questions:

- a) “Do small APs with diameters below 0.03-0.05 μm exist in the maritime tropical atmosphere, and if yes, what is their concentration?”
- b) Is the supersaturation in deep maritime clouds high enough to activate these smallest APs?

According to Twomey and Wojciehowsky (1969), Hegg and Hobbs (1992), Hegg et al (1993), Pruppacher and Keltt (1997) and Levin and Cotton (2009), the concentration of activated CCN in the maritime atmosphere increases monotonically with the increase in S_w up to the values as high as 8-10% (no measurements were performed at S_w higher than these values). The minimal diameter of soluble CCN that can be activated at S_w of 10 % is about 0.006 μm . It is a general practice to describe the dependence of CCN concentration using a semi-empirical formula

$$N_{cen} = N_o S_w^k, \quad (1)$$

where N_{cen} is the concentration of activated AP at supersaturation S_w (in %) with respect to water, N_o and k are the measured parameters. Parameter k is known as the slope parameter. The values of k vary from 0.3 to 1.3 within a wide range of supersaturations in different zones of the ocean (see Pruppacher and Keltt 1997), and even within different air masses in the same geographical location (Hudson and Li 1995). According to Pruppacher and Klett (1997) the averaged value of k for all maritime clouds is close to 0.9 which indicates the existence of a significant amount of small CCN in the maritime atmosphere. According to Levin and Cotton (2009) the typical value of k is close to 0.3, which also indicates the existence of small CCN, but with lower concentration than for data reviewed by Pruppacher and Klett (1997). Note that the data from Levin and Cotton (2009) corresponds to very remote maritime conditions.

At the same time, in some observational (e.g. Hudson 1984; Hudson and Frisbie 1991; Hudson and Li 1995; Hudson and Yum, 1997, 2002) and laboratory studies (Jiusto and Lala 1981) a decrease in the value of k with increasing S_w was reported. According to these results, no new CCN can be activated at supersaturations exceeding some threshold S_{thr} which is

assumed to vary from 0.1 % (Cohard et al, 1998; Emde and Wacker 1993) to about 0.6% (Hudson and Li 1995). Such observations connote a lack of small CCN with dry diameters lower than 0.05-0.12 μm in the sampled air, as seen sometimes for example in the remote maritime boundary layer (e.g., Clarke and Kapustin 2002). The $k(S)$ dependence with the condition that $k \approx 0$ at $S > S_{thr}$ is used in several studies (e.g., Cohard et al 1998; Abdul-Razzak et al. 1998) for parameterization of aerosol activation in cloud models. Hudson and Yum (2002) showed that the concentration of small aerosols is very low under clean Arctic conditions, while it is high enough in the Florida maritime air masses.

Despite this evident uncertainty, the observations of bimodal DSD spectra, high concentrations of ice crystals and large optical depths of deep tropical cloud anvils are consistent with the existence of small CCN that can be activated under S_w larger than several percent. Indeed, such small aerosols <15 nm have been directly observed in the free troposphere over the remote Pacific (Clarke and Kapustin 1992). The existence of small CCN follows also from the CCN budget. According to results of many studies (Twomey, 1968, 1971; Radke and Hobbs, 1969; Dinger et al. 1970; Hobbs, 1971; Levin and Cotton 2009) sea spray contributes mainly to the large AP tail of the AP size distribution, but most CCN in the accumulation mode are formed by collisions of smaller aerosols having another source different from the sea spray. The small CCN (belonging to the Aitken mode) can be of continental nature (e.g. from fossil fuel combustion or like Saharan dust, which is typically slightly hygroscopic [e.g. Twohey et al. 2009] and often was found in convective storms near the Eastern African coast and in storms and hurricanes reaching the American coast) or can form via various chemical reactions over the sea (Covert et al. 1992; Hobbs 1993; Pruppacher and Klett 1997, Clark and Kapustin 2002). The presence of significant concentrations of CCN with diameters ranging from 0.001 μm to 0.06 μm in the marine atmosphere was reported by Jaenicke (1993).

Many numerical simulations of aerosol effects on cloud microphysics, dynamics and precipitation (e.g., Takahashi 1984; Wang *et al.* 2005, van der Heever *et al.* 2006, Khain 2008; Tao *et al.* 2007, Phillips *et al.* 2001, 2002, 2005, 2007, 2009) (see overview by Khain 2009 for more references) have been carried out under different CCN concentrations typical of maritime and continental conditions. In most studies, the parameter N_o is usually varied within a wide range between a few tens and several thousand per cm^3 . The role of the slope parameter is

typically not discussed, and implicitly its role is assumed not to be decisive. In some of these studies the slope parameter was assumed to decrease with increasing S_w , which substantially decreases the efficiency of in-cloud nucleation. Besides, in many bulk-parameterization microphysical schemes and cloud parameterization used in global circulation models, nucleation of cloud-droplets is assumed to be restricted to the cloud base level.

The main goal of the present study is to show that small CCN can dramatically modify the microphysics and dynamics of maritime deep convection, where the supersaturation can be very high in its fast or precipitating convective updrafts. It will also be shown that in maritime clouds the combined effect of the smallest CCN and GCCN is to increase the concentrations of supercooled droplets aloft and of ice crystals in cloud anvils. At last, the idealized cases are considered to simulate the development of deep clouds within polluted air, such as clouds observed by Heymsfield et al. (2009) near the western coast of Africa. Numerical simulations are performed using an updated version of the Hebrew University Cloud model (HUCM).

2. Model description

The HUCM is a 2-D mixed-phase model (Khain and Sednev 1996; Khain et al 2004, 2005, 2008a) with spectral bin microphysics based on solving a system of kinetic equations for size distribution functions for water drops, ice crystals (plate-, columnar- and branch types), aggregates (snow), graupel and hail/frozen drops, as well as AP. Each size distribution is described using 43 doubling mass bins, allowing the simulation of hailstones with diameters up to 6.8 cm. The minimum particle mass is equal to that of a droplet with a radius of $2 \mu m$. The radii of dry AP serving as CCN range from $0.001 \mu m$ to $2 \mu m$. Ice particles are characterized by their mass and shape. To improve the representation of melting as well as riming by snow, several auxiliary size distributions have been recently introduced: a) distributions of liquid water mass within snow, graupel and hail; and b) distributions of rimed masses in snowflakes.

The model is specially designed to take into account the AP effects on the cloud microphysics, dynamics, and precipitation. *The initial* (at $t=0$) CCN size distribution is prescribed. At $t>0$ the prognostic equation for the size distribution of non-activated CCN is solved. Using the S_w values, the critical CCN radius is calculated according to Kohler theory. CCN with radii exceeding the critical value are activated and new droplets nucleated. The corresponding bins of the CCN size distribution then become empty.

Primary nucleation of each type of ice crystals is performed within its own temperature range following Takahashi *et al.* (1991). The dependence of the ice nuclei concentration on supersaturation with respect to ice is described using an empirical expression suggested by Meyers *et al.* (1992) and applied using a semi-lagrangian approach (Khain et al 2000) allowing the utilization of the diagnostic relationship in the time dependent framework. Production of secondary ice is treated according to Hallett and Mossop (1974). The rate of drop freezing is represented following the observations of immersion nuclei by Vali (1994), and homogeneous freezing according to Pruppacher (1995). The homogeneous freezing takes place at temperatures of about -38°C . The diffusional growth/evaporation of droplets and the deposition/sublimation of ice particles are calculated using analytical solutions for supersaturation with respect to water and ice. To increase the accuracy of calculation of supersaturation the equation for diffusion growth/evaporation was calculated using a variable time step which was decreased in some cases down to 0.1 s. An efficient and accurate method of solving the stochastic kinetic equation for drop collisions (Bott, 1998) was extended to a equation system calculating water-ice and ice-ice collisions. The model uses height-dependent drop-drop and drop-graupel collision kernels following Khain et al, (2001) and Pinsky et al (2001). To calculate turbulent-induced enhancement factors for collisions between droplets, the values of dissipation rate and Reynolds number were calculated in each grid point and at each time step. These values were used to calculate collision enhancement factors between droplets using lookup tables presented by Pinsky et al. (2008). As a result, the temporally and spatially dependent collision kernels between droplets were used for simulation of raindrop formation. Ice-ice collection rates are assumed to depend on temperature (Pruppacher and Klett, 1997). A detailed melting procedure with calculation of liquid water fractions within melting aggregates, graupel and hail is included following Phillips et al. (2007b). In order to control the transition of snow (aggregates) to graupel by riming snow the bulk density was calculated in each mass bin. If the bulk density exceeded 0.2 gcm^{-3} , i.e. became close to that of graupel, the snow from this bin was converted into graupel with the bin of the same mass.

To determine the snow bulk density in each mass bin, the rimed fraction of snow in each bin has been recalculated at each time step. The implementation of time- and space-dependent bulk-density of snow required re-calculation of the collision kernels because of changes in particle size and fall velocity. The fall velocity of rimed snow was calculated by interpolation between dry snow velocity and hail velocity of the same mass proportionally to the bulk density.

In the present model version, bulk density of graupel was set equal to 0.4 g/cm^3 which is the mean graupel density observed in cumulus clouds (Pruppacher and Klett 1997). Gradual changes of bulk density of graupel during riming will be accounted for in the next model version.

Advection of scalar values is performed with the positively defined conservative scheme proposed by Bott (1989).

The model was tested against many observations. For instance, it reproduces evolution of size distributions with height measured in situ in the field experiment in Amazon region (LBA-SMOGG) (e.g., Khain et al 2008, 2010c). These results can serve as validation of the model . The main focus of the study is the description of fine processes of formation of supercooled droplets and ice crystals at the upper cloud levels.

3 The experimental design

All runs were performed with a 2D computational domain is $26.5 \text{ km} \times 16 \text{ km}$, and a grid spacing of 50 m in both the horizontal and vertical directions. This resolution is close to that used in "Large Eddy Simulation" (LES) models and allows simulation of supersaturation and its variations with high accuracy.

The main goal of simulations was to investigate effects of small CCN which can be activated at supersaturations exceeding 1%. Two main sets of simulations are considered. The purpose of the first set of simulations is to investigate the role of small CCN in creation of supercooled water droplets at upper cloud levels and high concentration of ice crystals in cloud anvils of deep convective clouds. In this set of simulations the value of N_o was assumed equal to 100 cm^{-3} as is typical of maritime convection. The value of slope parameter k was assumed equal to 0.9. To show the role of the smallest CCN results of two simulations will be compared below: 1) maritime small-CCN case referred to as E100_S and 2) maritime no-small CCN case referred to as E100_NS (where S denotes existence of small CCN, while NS denote lack of the smallest CCN). In E100_S run, the minimal CCN radius was assumed equal to $0.002 \text{ }\mu\text{m}$, while in E100_NS the minimum CCN radius was assumed equal to $0.0124 \text{ }\mu\text{m}$, which corresponds to the absence of CCN at $S_w \geq 1.1\%$.

In order to investigate the combined role of the smallest CCN aerosols and GCCN, an additional simulation E100_SG was performed in which the CCN size distribution was similar to that in

E100_S at one exception: the concentration of GCCN with radii exceeding $1 \mu\text{m}$ was increased to be three times as large as that in E100_S.

The purpose of the second set of simulations was to investigate effects from small CCN in clouds developing in polluted air. In these simulations N_o was assumed equal to 3500 cm^{-3} and slope parameters of $k=0.9$ and $k=0.3$ were used. Corresponding simulations are referred to as E3500_k09 and E3500_k03, respectively.

The maximum dry CCN radius in the model is $2 \mu\text{m}$. These largest CCN give rise to wet particles (droplets) of $8 \mu\text{m}$ in radius at 100% relative humidity. No GCCN with dry radii larger than $4 \mu\text{m}$ were allowed. The initial size distributions of CCN in all simulations are depicted in **Figure 2**. The initial aerosol concentration was assumed constant within the lower 2-km layer and decreased with height exponentially above it with a characteristic spatial scale of 1.5 km.

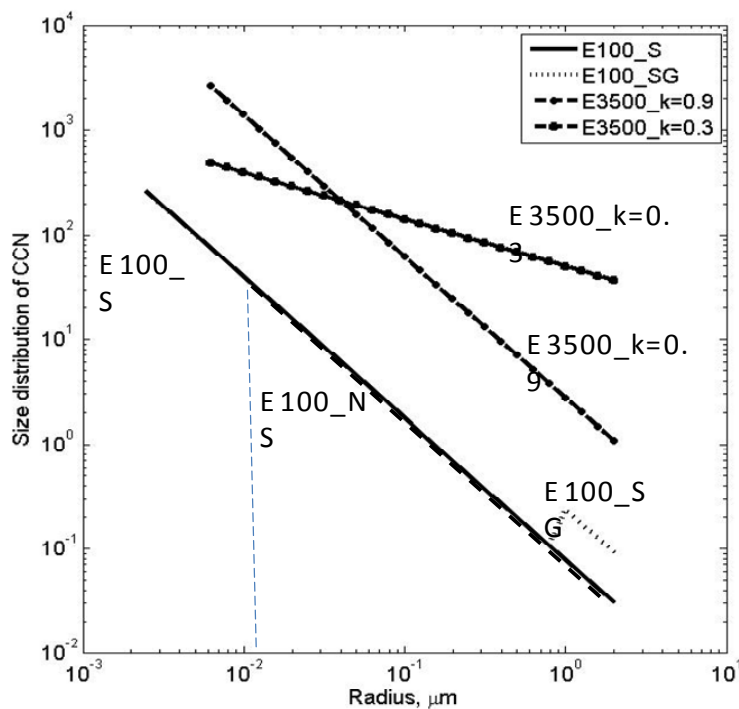


Figure 2. Size distributions of aerosols in different simulations

We would like to mention that in some studies (e.g. Warner 1973) the formation of bimodal DSDs is attributed to mixing of clouds with their environment. In the study by Warner (1973), such results were obtained using 1-D Lagrangian parcel model, when effects of mixing

immediately affected the microphysics of the entire cloud. In a multi-dimensional model with realistic dynamics the situation is more complicated. Note that the model design allows both mixing of clouds with environment and lateral penetration of CCN into clouds at higher levels. Moreover, advection of CCN by the velocity field can increase the concentration of CCN (including small CCN) at upper levels. It means that the aerosol and dynamical conditions of E100_NS do not exclude the possibility of in-cloud nucleation at significant distances above cloud base. We just hypothesize that small CCN ascending from the cloud base play the major role in production of supercooled droplets and ice crystals in cloud anvils. This expectation agrees with observations of Heymsfield et al (2009) that the maximal concentrations of supercooled droplets and crystals formed by homogeneous freezing are located in vicinity of cloud axes, and with previous modeling results from Phillips et al. (2005) noted above.

Estimations of the propagation velocity of aerosols due to turbulent diffusion show that aerosols from lateral cloud boundaries hardly can reach the cloud core of a convective clouds of several km in width during the time of air ascent from the cloud base to the cloud top (e.g. Khain et al 2004).

As the basis for the thermodynamic sounding, the sounding observed during Day 261 of GATE 1974, as applied in many simulations of deep tropical convection, was used (e.g. Ferrier and Houze 1989). Such a sounding resembles those typical of tropical oceans during hurricane season (Jordan 1958). The sounding indicates 90 % humidity near the surface. The freezing level is at 4.2 km. The atmosphere is relatively unstable under these conditions, so the maximum vertical velocity in the simulated clouds is about 18 m/s. However, to simulate especially strong maritime clouds with vertical updrafts of 25 m/s at ~10 km height, which produce crystals at the high concentrations reported by Heymsfield (2009), the profile of dew point was changed as shown in **Figure 3** by dashed line.

These convective clouds fall into the range of the 5% of the most intense maritime clouds according to Jorgensen et al. (1985) and Jorgensen and LeMone (1989). Wind shear was assumed equal to 2m/s per 10 km layer. Above the 10 km altitude, background wind was assumed to be 2m/s. Clouds were triggered using a temperature heating of a triangle form with a maximum of 0.005 °C/s in the center of the model domain within the layer between 50 m and 2 km levels. The horizontal extension of the heating zone was 2 km, and the duration of heating is 1200 s. It is clear that such convective triggering is idealized. Deep convective cloud in the tropics and eyewalls of

TCs, are triggered dynamically by air convergence in the boundary layer caused by downdrafts of neighboring clouds or by some other reasons. However, for the model geometry used, the utilization of the initial heating is simpler. The main requirement with such heating is to create updrafts at cloud base of a few m/s in agreement with the speeds observed in a vigorous maritime convective clouds observed during Tropical Ocean and Global Atmosphere Coupled Ocean_Atmosphere Response Experiment (TOGA COARE) (Fierro et al 2009; Heymsfield et al 2009) .

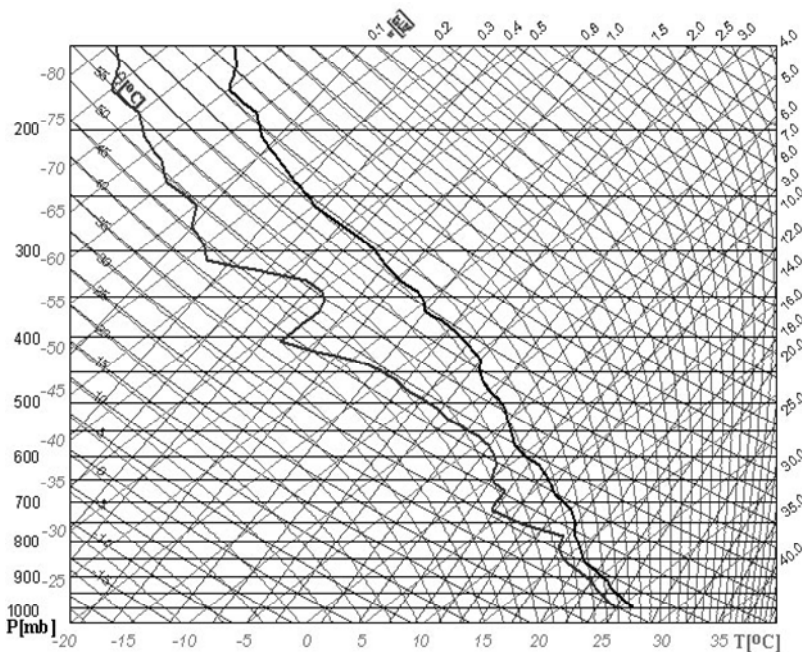


Figure 3. Vertical profiles of temperature and dew-point used in simulations.

4. Results of simulations

4.1 Role of small CCN

In this section we will compare results of simulations E100_S and E100_NS (in the latter ran the CCN size distribution does not contain CCN with diameters lower than $0.025 \mu m$). During the first 20 min of cloud evolution the fields of droplet concentration N_d , cloud water content CWC (droplets with the radii below $40 \mu m$), rain water content (RWC), and vertical velocity W are quite similar between these simulations. The cloud base is located at about 1 km altitude. The maximum N_d are $\sim 110 cm^{-3}$, the maximum CWC reaches $2.4 g m^{-3}$, rain forms at 2.5 km level, i.e. 1.5 km above the cloud base. Collection of cloud droplets by raindrops

decreases N_d and CWC substantially at ~ 3 km level. When this happens, the monotonic decrease in N_d and CWC with height ceases. The mechanism of this effect is illustrated in **Figure 4**, which depicts the fields of cloud-droplet number concentration, RWC, W and S_w in E100_S at $t=1860$ s.

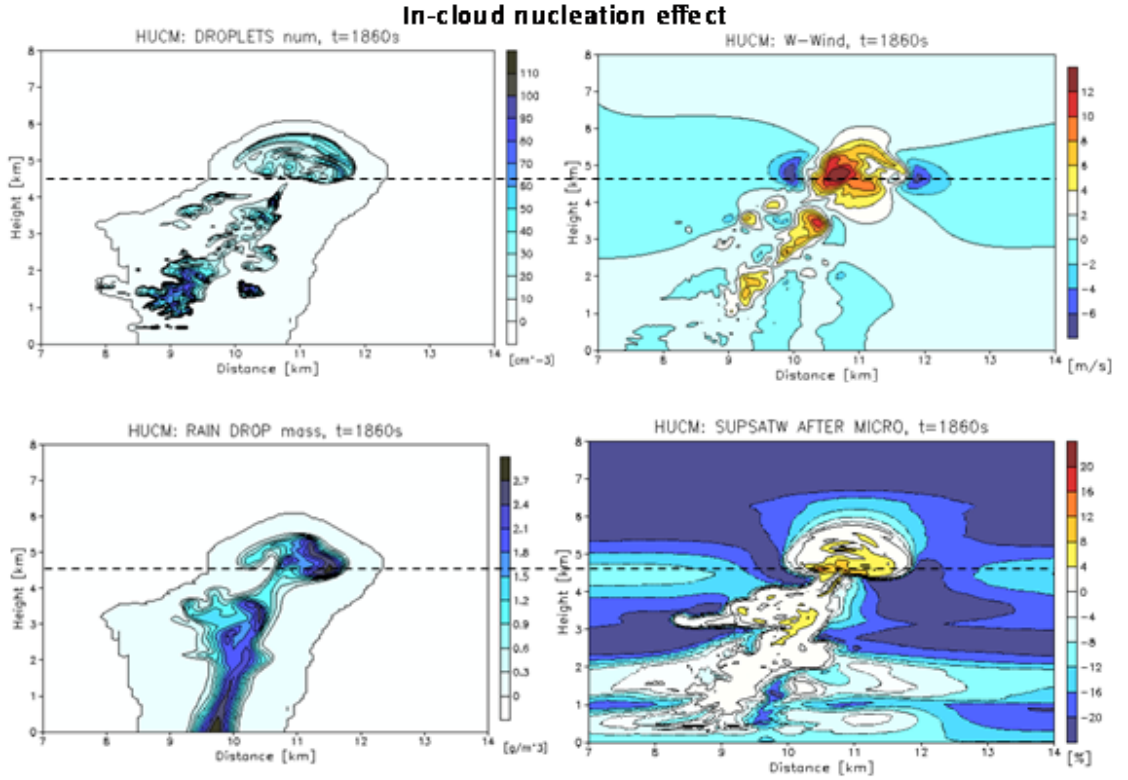


Figure 4 Fields of CWC, RWC, W and supersaturation at $t=1860$ min in E100_S simulation

Figure 5 (left panels) shows the CWC. One can see that the zone of new CWC arises just above 4.5 km. The zone of new CWC is located slightly above the level of the RWC maximum, and coincides with a sharp increase of vertical velocity with height up to 10 m/s at 5 km altitude. This increase in vertical velocity is likely caused by rain unloading. The increase in the vertical updrafts above ~ 5 km level is the typical feature of maritime clouds (e.g. Petersen et al. 1999). Maximum S_w in this region exceeds $\sim 8-10\%$. Such high values of S_w are not unusual (which is especially true in maritime clouds). The existence of such high supersaturations follows from the theory for an adiabatic parcel ascent (e.g., Rogers and Yau 1989; Korolev and Mazin, 2003; Korolev 2007) according to which S_w rapidly reaches the equilibrium value $S_{eq} \sim W / (N_d \bar{r}_d)$

(where \bar{r}_d is the mean droplet radius). For instance, at $N_d \sim 5\text{cm}^{-3}$ (in the zone of efficient collisions and just above it), $\bar{r}_d \sim 20\mu\text{m}$ and $W \sim 12\text{ m/s}$ supersaturation may even exceed 15%-30% (Korolev and Mazin 2003). According to the Kohler law, at a value of S_w of 10 %, the soluble CCN with dry diameters as low as $0.006\ \mu\text{m}$ are activated. Accordingly, in-cloud nucleation takes place above 4.4 km altitude.

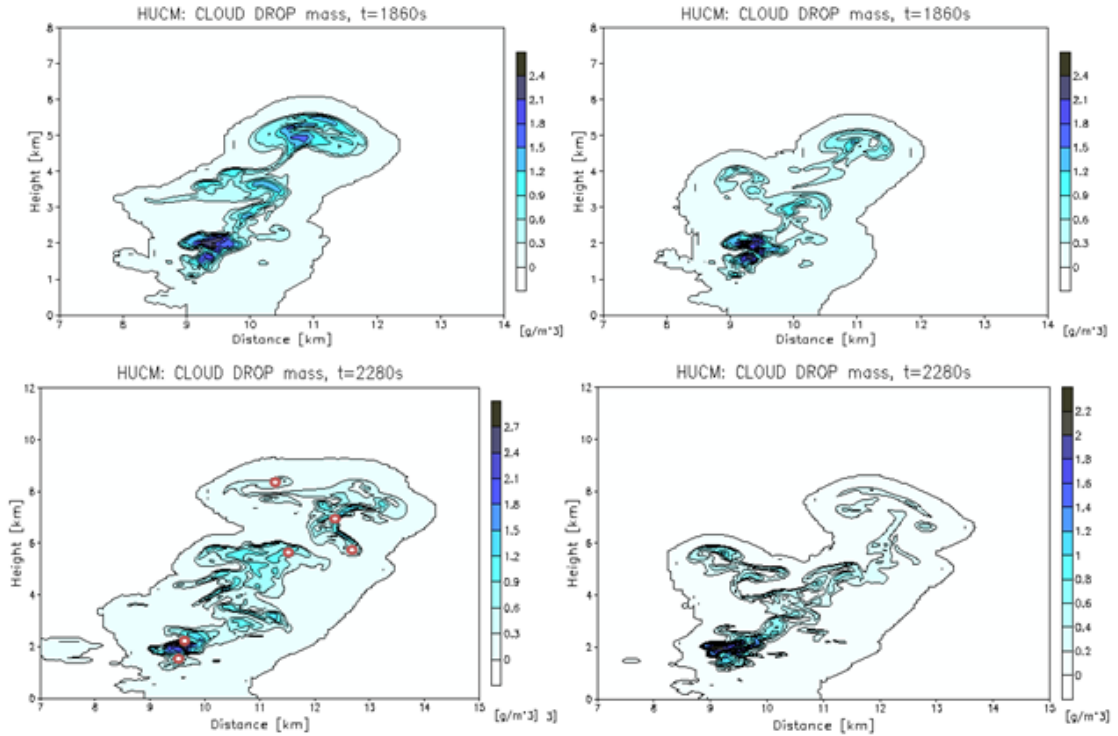


Figure 5 Fields of CWC in E100_S (left) and E100_NS (right) at 1860 and 2280 s.

In the E100_NS the absence of CCN with diameters $0.025\ \mu\text{m}$ does not allow nucleation of significant amount of cloud-liquid. The absence of intense in-cloud nucleation leads to the increase in superstaration to $\sim 30\%$ in this run (not shown). The difference in CWC fields in these runs increases with time (**Figure 5**). One can see that whereas in the E100_S run the regions with a significant CWC arise within the 6-8 km layer. In the E100_NS the CWC above 6 km is much smaller.

Figure 6 shows droplet size distribution (DSD) in different points in the cloud in E100_S. These points were marked by circles in **Figure 5**. One can see the existence of droplets with diameters as low as $5\ \mu\text{m}$ at many cloud levels. New droplets with diameters as small as $5\ \mu\text{m}$

arise at $z=5.8$ km. At height of 8.5 km the DSD again contains small droplets with diameters of $5 \mu\text{m}$, while such droplets were absent at 6.75 km. We see, therefore, that the process of in-cloud nucleation is widespread in maritime clouds, at least as it follows from these simulations. Note in this connection a very important result about the values of supersaturation in mixed-phase clouds formulated by Korolev and Mazin (2003), namely: the equilibrium supersaturation is determined by the liquid phase. Since the riming decreases concentration of supercooled droplets, it should lead to an increase in supersaturation. It means that the conceptual picture of in-cloud nucleation presented in **Figure 1** should be extended to the mixed-phase case, when droplet concentration decreases and supersaturation increases as a result of riming during ascent.

Note that newly nucleated droplets rapidly grow at high supersaturations. As a result, the gaps between different modes seen in **Figure 1** disappear and DSDs become comparatively wide unimodal DSD with a relative dispersion of 0.2-0.4, despite the presence of in-cloud droplet nucleation.

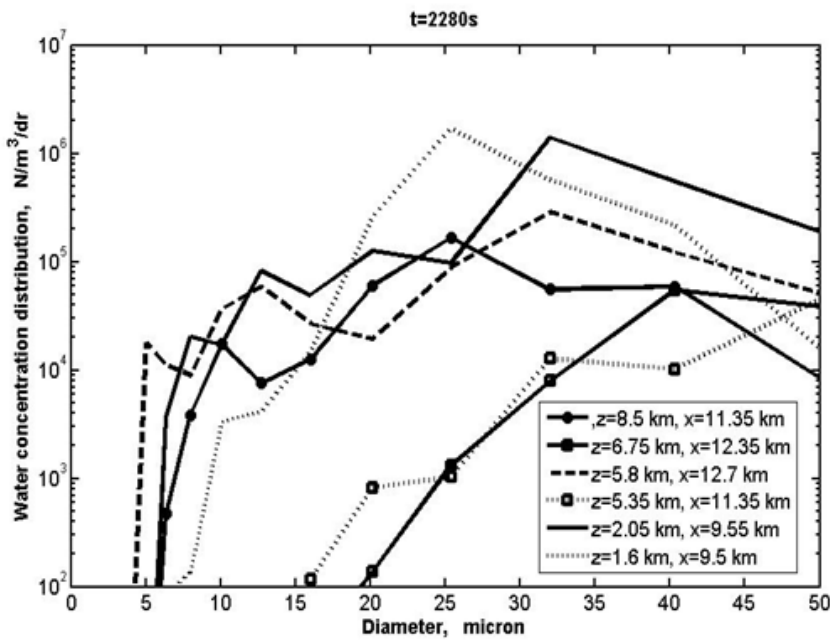


Figure 6. Droplets size distributions in E100_S at $t=2280$ s in points marked in Figure 5 by circles

Figure 7 shows vertical profiles of maximum values of N_d , LWC , total ice content and ice crystal concentration in clean air simulations with small CCN included (E100_S), with no-small CCN (E100_NS) and in the presence of both small and GCCN (E100_SG). The profile of

$N_{d\max}$ indicates several peaks corresponding to zones of in-cloud nucleation. Droplet concentration in E100_S is larger than in E100_NS. For the purposes of the present study, it is of importance that the droplet concentration in E100_S increases with height above the 8-km level, while the concentration in E100_NS rapidly decreases with height above 8 km. Note that observations of Heymsfield *et al* (2009) indicate the increase in $N_{d\max}$ above 8-km level. We attribute the in-cloud nucleation above ~ 8 km level to the decrease in droplet concentration by riming as was discussed above. Liquid water content is also larger in E100_S than in E100_NS and decreases with height above the level of 4 km. A rapid decrease in LWC above 6 km can be attributed to riming by collisions of water drops with ice particles of various kinds. The total mass ice content has its maximum at 8 km. Vertical profiles of ice crystal concentration reveal a dramatic difference between E100_S and E100_NS: whereas the peak of the time-averaged concentration of ice crystals at about 10 km altitude is 6.5 cm^{-3} in E100_S, it is about 1 cm^{-3} in E100_NS. This is due to fewer supercooled droplets in the upper half of the mixed-phase region when the smallest aerosols are not present, so that homogeneous freezing is drastically reduced.

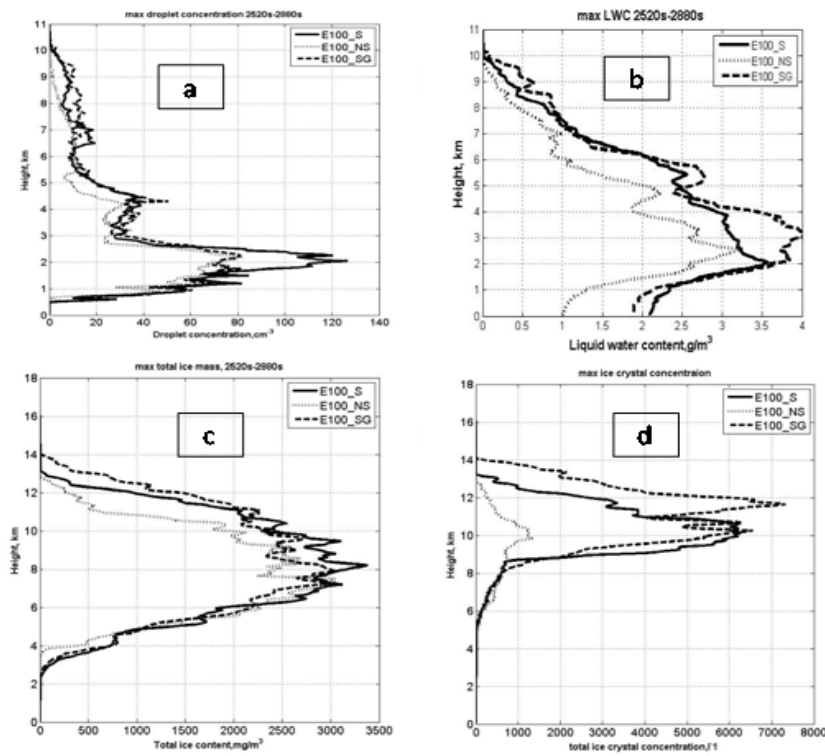


Figure 7. Vertical profiles of maximum values of droplet concentration (a), LWC (b), Total ice content (c) and ice crystal concentration (d) in simulations with low CCN concentration. The profiles are averaged over the time period between 2520 and 2880 s.

As was discussed above (Sect. 3) the conditions of E100_NS do not exclude the possibility of in-cloud nucleation altogether, but just significantly decreases its intensity and probability (compare, for instance, Fig. 5c and 5d-2280s). **Figure 7a** indicates also some increase in the droplet concentration with increasing height above 3.5 km altitude in this run. There are several reasons for this. First, only CCN with radii below $0.0125 \mu m$ are eliminated in E100_NS. Besides, the simulations with resolution of 50 m reproduce separate bubbles in cloud structure which ascend along different trajectories and have different histories of supersaturation. Moreover, CCN are transported by the velocity field, so that small CCN can ascend from below, say 2 km altitude (i.e. above cloud base), upward and may penetrate cloud bubbles at higher levels (or produce new cloud elements by activation). The main conclusion of the present study, however, is that the concentration of supercooled droplets in E100_S is significantly higher than in E100_NS which indicates the role of small CCN in production of supercooled droplets and ice crystals.

Figure 8 shows the fields of plate-like crystal concentration in E100_S (a), E100_NS (b) and E100_SG (c) at $t=2760$ s, when cloud top is above 10 km (the level of homogeneous freezing). One can see a dramatic difference in the ice crystal concentrations in cases of significant and low amounts of small CCN in the CCN activity spectrum. The area covered by ice crystals in E100_S is also larger than in E100_NS. Panel (d) shows time dependence of maximum concentration of plate crystals (forming by homogeneous freezing) in these simulations. One can see that cloud reaches the level of homogeneous freezing in E100_S earlier than in E100_NS, and ice crystal concentration in E100_S is substantially larger during the entire simulation.

Analysis of size distribution of plate-like crystals in several points at levels between 10 and 11 km shows that maximum concentration of crystals is reached at diameters of about $70 \mu m$, indicating that these crystals are comparatively small (in agreement with observations by Heymsfield et al 2009).

4.2 The combined effect of small and giant CCN

As was discussed above (Sec.1), GCCN accelerate the warm rain formation. In case the CCN spectrum does not contain small CCN, i.e. all CCN are activated at cloud base, the increase in GCCN concentration should decrease the supercooled liquid content aloft, and weaken the efficiency of ice processes. **Figures 7** and **8** show that in the presence of small CCN, the effects

from GCCN turn out to be just opposite of that usually assumed. Being included into the DSD the GCCN accelerate formation of warm rain, leading to a sharper decrease in the droplet

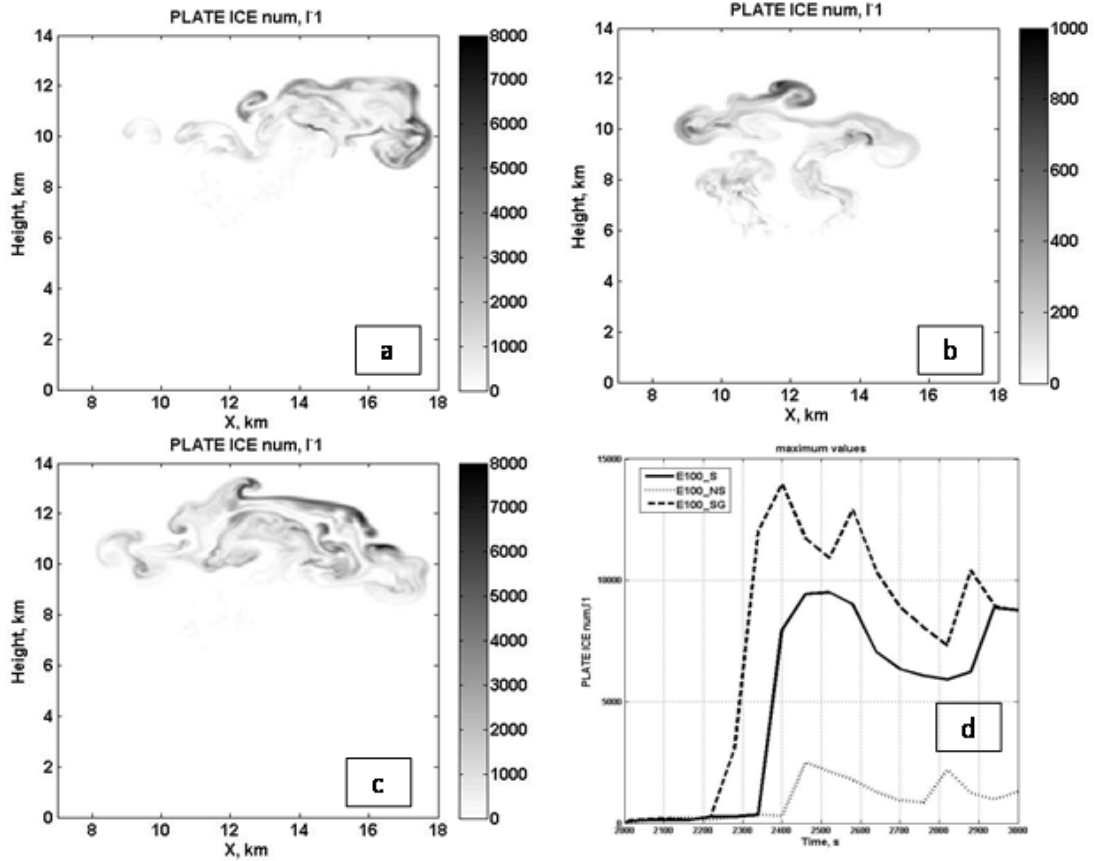


Figure 8. Fields of plate-like crystal concentration in E100_S (a), E100_NS (b) and E100_SG (c)

concentration during ascent and more rapid unloading of rain. Both factors lead to the increase in supersaturation, which in the presence of small CCN leads to intensification of in-cloud nucleation. As a result the increase in concentration of GCCN boosted the supercooled water content below the level of homogeneous freezing and, accordingly, the concentration of ice crystals too above the homogeneous freezing level (about 10 km altitude).

4.3 Effects of small CCN on the lightning probability

Figure 9 depicts lightning potential (LP) (evaluated as accumulated number of collisions between ice crystals and graupel per unit of volume) in E100_S; E100-NS and E100_SG. The graupel-ice crystal collisions at particular time step were taken into account if supercooled LWC

in this grid point exceeded 0.1 g m^{-3} . **Figure 14d** shows the evolution of lightning potential in all simulations. We would like to stress here that detailed simulation of the processes of charge separation and lightning formation was beyond the scope of this paper. Therefore, the values of lightning potential can be interpreted only qualitatively. We assume just that larger values of AP correspond to higher rates of charge separation and a greater probability of lightning. The LP used in this study is quite similar to that successfully applied by Khain et al. (2010a) to characterize lightning location and intensity in a landfalling hurricane.

Comparison of the fields of LP calculated in the present study shows that small CCN increase the lightning probability by increasing the concentration of supercooled droplets, concentration of ice crystals and graupel.

Figure 9 shows also that the lightning potential in E100-SG is larger than in other simulations, because of reasons discussed above. We suppose that this result can explain the observed intense lightning in eyewalls of hurricanes during their mature stage, when production of GCCN is maximal and a huge amount of GCCN enters the clouds via cloud base.

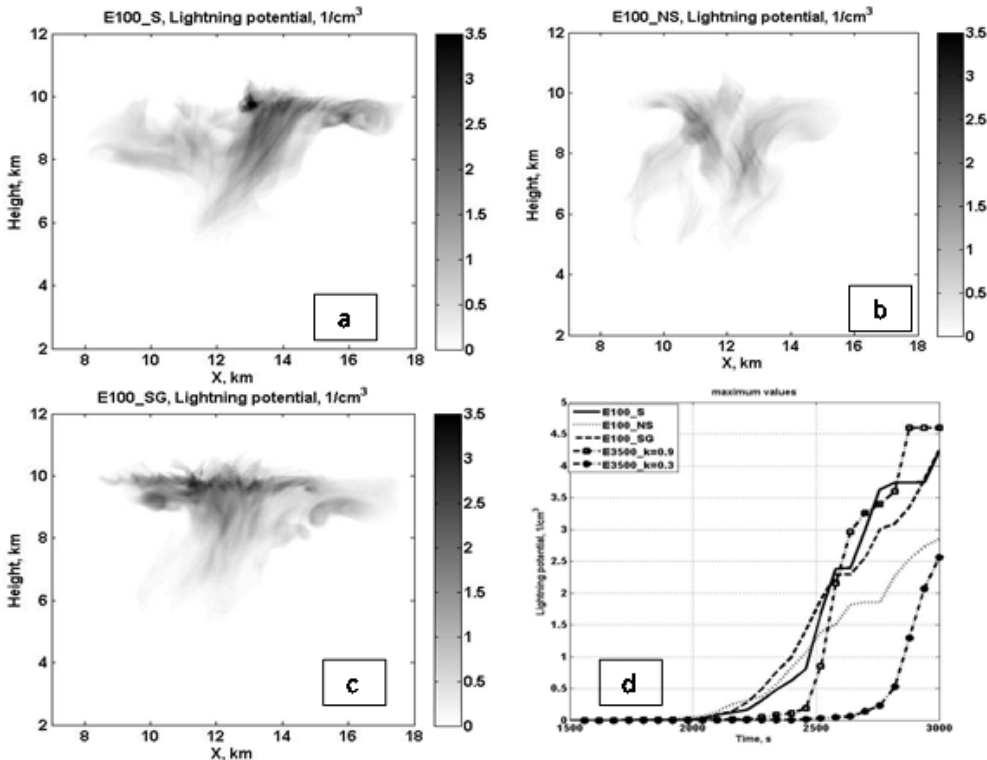


Figure 9 Lightning potential in E100_S (a), E100_NS (b) and E100_SG (c). Panel d shows time dependence of lightning potential in all simulations.

4.4 Effect of small AP on cloud microphysics of polluted clouds

Significant effects from the CCN concentration on microphysics and precipitation of tropical maritime clouds were investigated in many studies (Khain 2009). It was stressed that an increase in the CCN concentration augments the supercooled water content aloft, causing convective invigoration and intensified glaciation. However, the particular role of the smallest CCN was not specifically investigated. In this section we will compare the results in two simulations E3500_k03 and E3500_k09, which involved the same thermodynamic conditions as in the E100 simulations. In these simulations $N_0=3500 \text{ cm}^{-3}$, and slope parameters were equal to 0.9 and 0.3, respectively.

Supersaturation with respect to water in polluted clouds is lower than that in clouds developing in clean air. The lower supersaturation in polluted air causes a higher altitude of formation of the first raindrops, as is clearly seen in observations (e.g. Freud *et al.* 2008). Indeed, the simulations show that the supersaturation with respect to water in the polluted clouds does not exceed $\sim 1\%$ until the level of 5-7 km altitude is reached. However, in ascent above this level the process of riming leads to a decrease in CWC and droplet concentration. At the same time vertical velocities increase with height above the 7 km level. As a result, S_w grows above 7 km altitude, reaching $\sim 8\%$. These values of supersaturation are high enough to lead to in-cloud nucleation.

The existence of in-cloud nucleation is clearly seen in **Figure 10** showing vertical profiles of maximum droplet concentration (a), CWC (b), liquid water content (c) and total ice content (d) in simulations E3500_k03 and E3500_k09 at $t=3300\text{s}$. One can see that in E3500_k09 (where the amount of small CCN is higher) the concentration of droplets is less than in E3500_k03 below ~ 6 km altitude and significantly higher above 6 km. This behavior corresponds to the CCN distributions shown in **Figure 2**: in E3500_k03 the concentration of large CCN is higher, but the concentration of small CCN is higher than in E3500_k09. One can see a significant increase in droplet concentration above 6 km in E3500_k09 caused by in-cloud nucleation. In agreement with differences in the CCN spectra, LWC in E3500_k03 is larger than in E3500_k09 up to 9 km altitude largely due to the larger value of RWC.

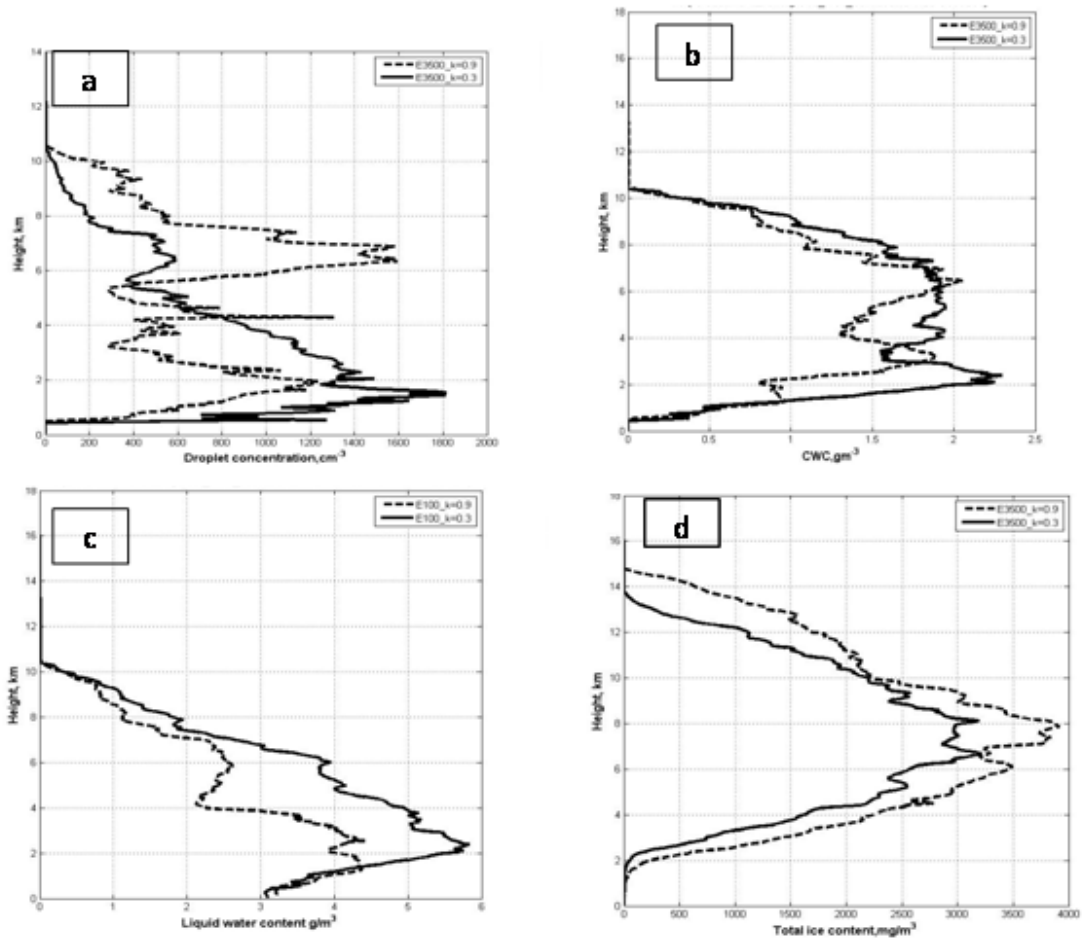


Figure 10. Vertical profiles of maximum droplet concentration (a), CWC (b), Liquid water content (c) and total ice content (d) in simulations E3500_k03 and E3500_k09 at $t=3300s$

Figure 11 shows fields of plate crystals concentration in E3500_k09 (left) and in E3500_k03 (right) at $t=3300s$. One can see that in E3500_k09 concentration of crystals is 350 cm^{-3} at 12 km, in agreement with measurements of Heymsfield et al (2009) in polluted clouds. In E3500_k03 the maximum concentration of ice crystals is 40 cm^{-3} .

Figure 12 shows mass contents of graupel and hail in these simulations. One can see that difference in CCN concentrations related to differences in slope parameters (k) affects microphysical fields. Comparison of hail contents in clean and polluted cases shows that hail forms largely in clouds developing in polluted air. Amounts of hail in simulations E100 were

negligible. At last, **Figure 9d** shows that the lightning potential in E3500_K09 is larger than in all other simulations. This $k=0.9$ case has a higher concentration of small CCN.

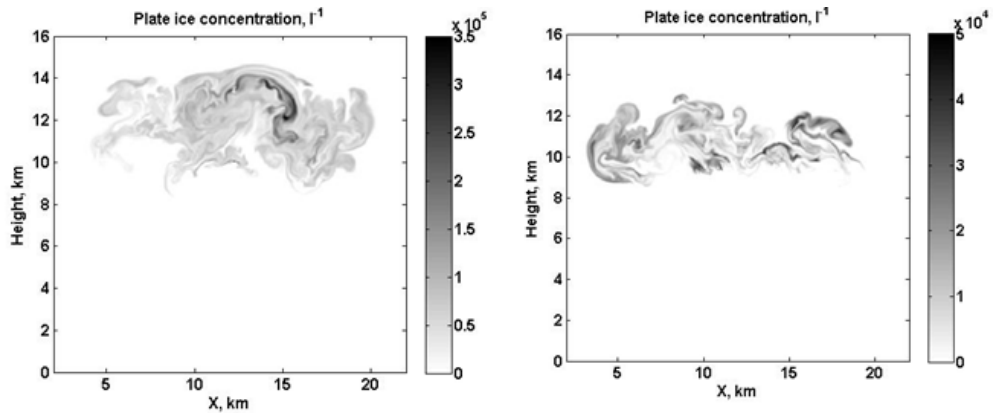


Figure 11. Fields of plate crystals concentration in E3500_k09 (left) and in E3500_k03 (right) at $t=3300s$. Note that scales in the panels are different.

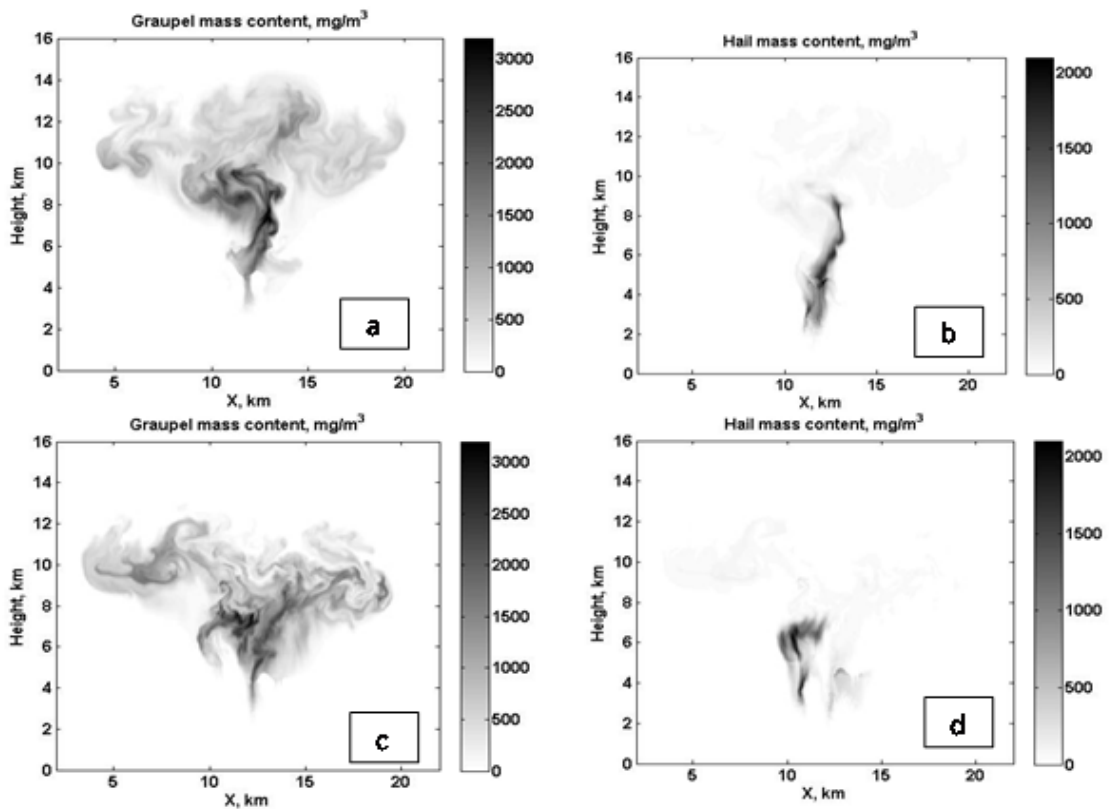


Figure 12. Fields of graupel mass contents (a,c) and hail mass contents (b,d) in E3500_k09 (upper low) and in E3500_k03 (bottom) at $t=3300s$.

4.5 Effect of small CCN on cloud dynamics, accumulated rain and radar reflectivity

Differences in concentration of small CCN lead to differences in cloud dynamics, microphysics and affects precipitation.

Figure 13 shows the vertical profiles of maximum vertical velocity in clouds developing in a clean atmosphere (a), and polluted air (b). The profiles are averaged over the time period of several minutes. One can see that small CCN increase the maximum speeds of the cloudy updrafts and increase the height level of the maxima by about 2 km. The profiles in runs with small CCN are taken into account and resemble those presented by Heymsfield et al. (2009), indicating the maxima also at 10 km level. In agreement with the results reported by Petersen et al (1999) vertical velocity in clouds developing in clean air increase strongly with height above ~ 5-6 km level.

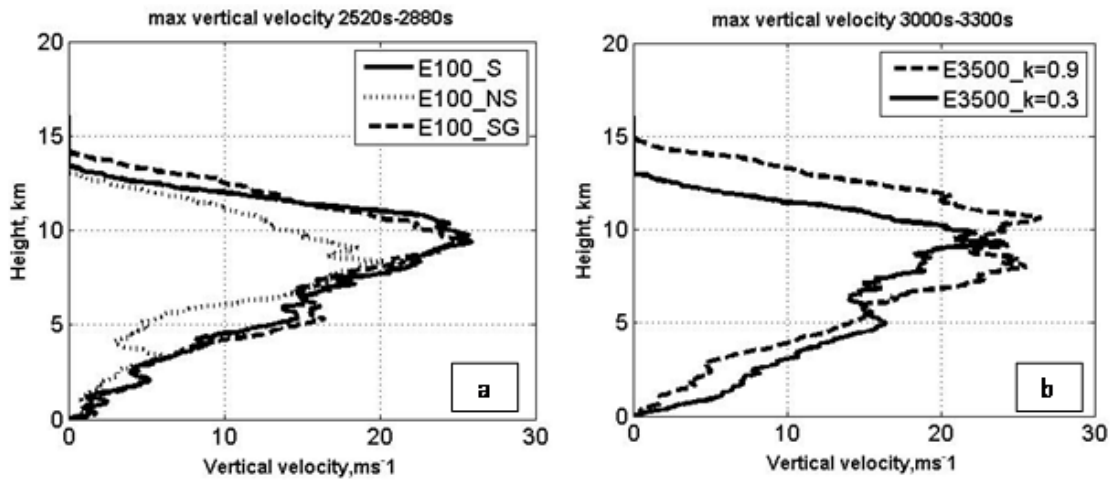


Figure 13. Vertical profiles of maximum values of vertical velocity in clouds developing in clean atmosphere (a), and polluted air (b). The profiles are averaged over the time period of several minutes.

Figure 14 shows the corresponding time dependencies of these maximum updraft velocities for clean air (left) and polluted air (right). One can see that maximum updraft speeds are typically larger in simulations having small aerosols in the CCN spectra. This can be attributed to larger latent heat release during the diffusional growth of droplets nucleated via in-cloud nucleation, as well as to higher total ice contents (formed by riming) in these cases. **Figure 15** depicts vertical profiles of maximum radar reflectivity from various simulations in clean (left) and polluted (right)

air. One can see that clouds developing in the case of high concentration of small CCN have larger reflectivity. Reflectivity in E100_S is significantly higher than that in E100_NS. It is interesting that the addition of GCCN in simulation E100_SG leads to an increase in reflectivity at upper levels, indicating larger masses of ice crystals and snow. The vertical behavior of radar reflectivity in E100_SG resembles that observed in eyewalls of hurricanes (Willoughby et al 1985). Radar reflectivity in polluted clouds is typically higher than that in clean air because of larger amounts of hail produced in polluted air. The increase in amount and size of hail in clouds developing in polluted air is discussed in detail in Khain et al (2010b). Clouds developing in polluted air contain more supercooled water at upper levels. As a result, the process of riming of hail embryos is more efficient in polluted air. Radar reflectivity is nearly constant over altitude below the freezing level and then decreases with increasing height above it. In polluted air, radar reflectivity decreases with height slower than in clean air, especially in cases when the CCN spectra contains higher amount of small CCN.

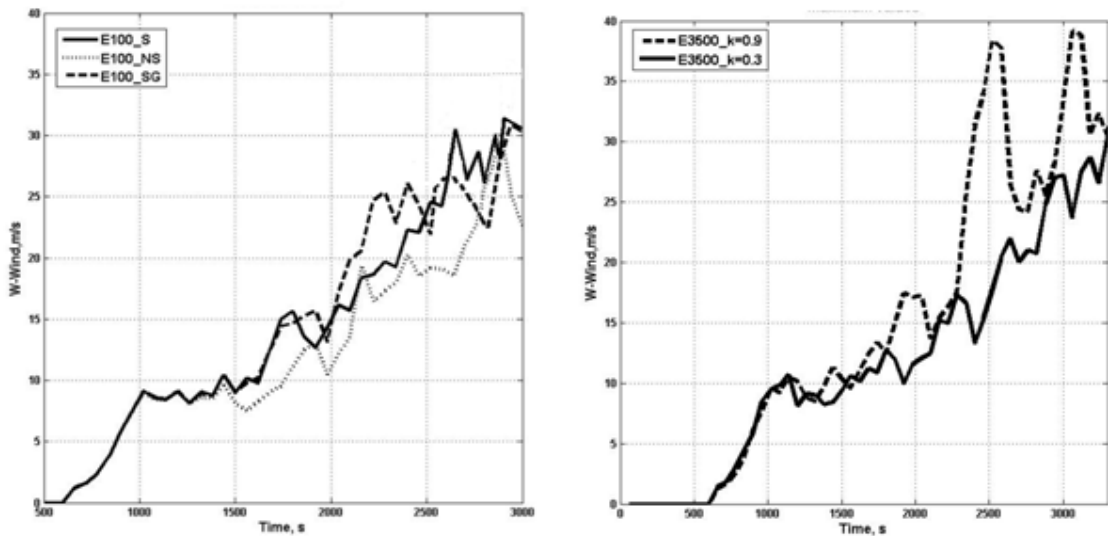


Figure 14. Time dependencies of maximum updraft velocities in simulations in clean air (left) and polluted air (right) in different simulations

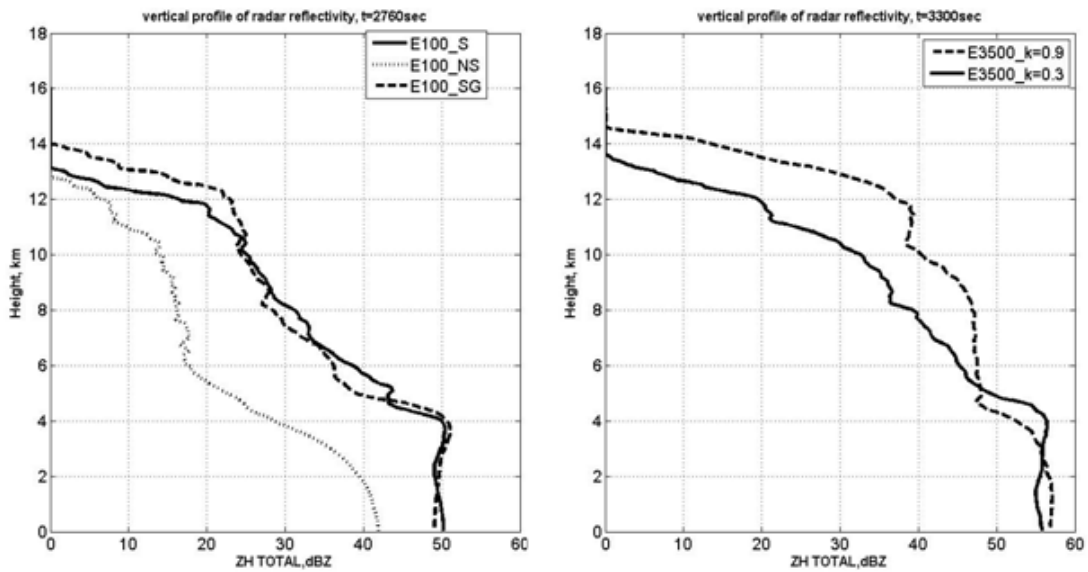


Figure 15. Vertical profiles of maximum radar reflectivity in in simulations in clean air (left) and polluted air (right) in different simulations

Figure 16 shows the evolution with time of accumulated rain in different experiments. One can see that in clean air, rain at the surface begins earlier because of faster formation by coalescence. Accumulated rain in polluted clouds turns out to be higher than that from clouds developing in clean atmosphere. This effect is discussed in detail in overview by Khain (2009). For the purposes of the present study, a more interesting result is that in the presence of small CCN in the aerosol size distribution leads to an increase in surface precipitation: accumulated rain in E100_S is larger than that in E100_NS. It is remarkable that additional amounts of GCCN increase accumulated rain in case the aerosol size distribution contains small CCN. This can be attributed to intensification of processes of in-cloud nucleation and ice processes at upper levels in E100_SG, as was discussed above.

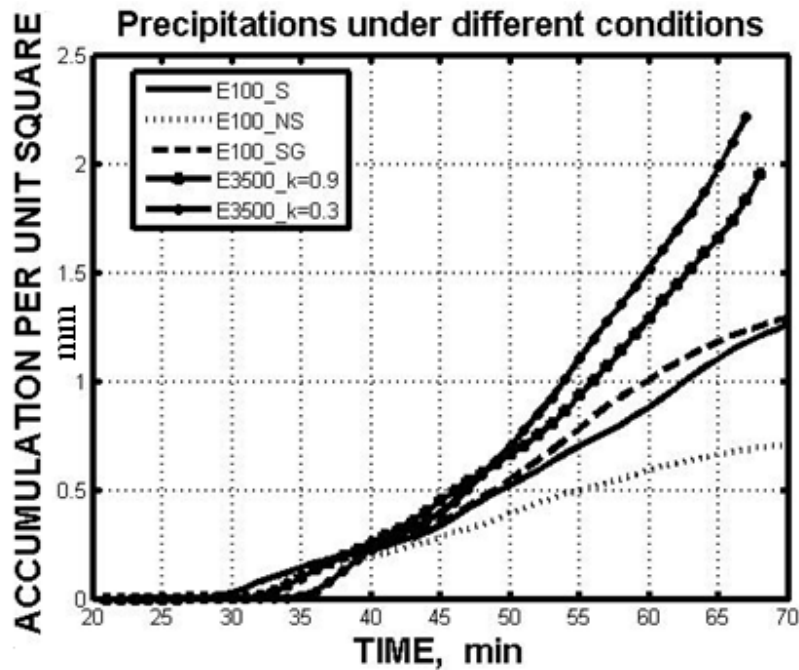


Figure 16. Time dependencies of accumulated rain at the ground in different experiments. See text for more detail

5. Discussion and Conclusions

This study was motivated by observations of very high concentrations of ice crystals in cloud anvils of especially strong maritime clouds. The existence of intense lightning in eyewalls of hurricanes in the presence of huge GCCN concentration also required an explanation. Simulations with a mixed-phase cloud microphysics model with a resolution of 50 m and accurate calculation of cloud supersaturation show that all these phenomena can be explained by in-cloud nucleation of small droplets at temperatures colder than -15°C to -20°C . It is shown that in maritime clouds, efficient production of warm rain leads to a decrease in droplet concentration aloft, which is often accompanied by an increase in vertical velocity (one of the reasons of such updraft acceleration is unloading of precipitation). As a result, supersaturation can exceed 10%-20% in maritime clouds. To be efficient, in-cloud nucleation requires the existence of a significant concentration of small CCN belonging to Aitken mode with diameters below $\sim 0.03\text{-}0.05\ \mu\text{m}$. It is shown that in case the vertical velocity in clouds reaches $\sim 25\ \text{m/s}$ at $z\sim 10\ \text{km}$, in-cloud nucleation of droplets, several km above cloud-base, can produce $\sim 5\text{-}15\ \text{cm}^{-3}$ ice crystals by homogeneous freezing of small cloud

droplets if the slope parameter $k=0.9$. Such a slope parameter is typical of maritime conditions according to Hobbs (1993) and Pruppacher and Klett (1997). Ice crystals of such concentration at anvil levels were measured in maritime clouds of corresponding intensity by Heymsfield et al (2009).

These conclusions are broadly consistent with the crucial role for in-cloud nucleation far above cloud-base evident from simulations by Pinsky and Khain (2002) and with their conceptual picture noted above (Sec. 1). They are also consistent with simulations by Phillips *et al.* (2005) that showed in-cloud nucleation of droplets far above cloud-base produced most of the supercooled droplets freezing homogeneously. It is usually assumed that the effects of small CCN and GCCN are opposite: while small CCN tend to delay the warm rain formation, GCCN act to accelerate it. According to this concept, the existence of GCCN should decrease amount of supercooled water at upper levels of maritime cumulus clouds. This concept is true if all CCN activation takes place in the vicinity of cloud base. In this study, it is shown that effects of very small CCN (which are not activated at cloud base and can be activated at supersaturations exceeding one to several percents) and GCCN can lead to a synergetic effect as regards formation of new droplets at higher levels via in-cloud nucleation. Fostering the formation of warm rain, which then is unloaded from the updrafts, making them faster, GCCN can lead to a higher supersaturation in clouds aloft and to greater production of supercooled droplets at upper levels via in-cloud nucleation. As a result, both the concentration of small droplets aloft and the concentration of ice crystals in cloud anvils forming by homogeneous freezing increases if the CCN spectrum at cloud base contains both Aitken CCN and GCCN.

The process of in-cloud nucleation allows one to explain formation of high concentrations of ice crystals, high optical depth of anvils of deep tropical clouds, and accompanying cirrus clouds in the ITCZ. It also explains the lightning in very strong convective clouds in the ITCZ over the oceans. The synergetic effect of the smallest CCN and GCCN allows one to explain the formation of lightning in extremely maritime clouds in eyewall of hurricanes.

In our simulations, which focus on the effects from the smallest CCN penetrating through cloud base, the roles both of vertical velocity and cloud depth are extremely important. In supplemental simulations (which were not discussed in the study) for which the original sounding was used, the maximum vertical velocity of 18 m/s was reached at ~9 km, but not 10 km. In this case the concentration of ice crystals in cloud anvils was an order of magnitude less than in the

case with a maximum of vertical velocity of 25 m/s at 10 km. The lightning potential was lower accordingly. In supplemental simulations, in which relative humidity was decreased to get a maximum vertical velocity of 10-13 m/s, concentration of ice crystals in cloud anvils was $\sim 100 \text{ l}^{-1}$, being produced largely by primary ice nucleation. The concentration of supercooled droplets above 8 km was negligible. In such simulations cloud top was at about 10 km altitude or lower and lightning potential was negligibly small. This is in agreement with findings by Black and Hallet (1999) showing that lightning in hurricane clouds is possible if the vertical velocity exceeds 13 m/s.

Note that two main hypotheses as regards the main factors leading to lightning are widely discussed in the literature: the "dynamical" and "aerosol" hypotheses. In the first case, the vertical velocity is considered as the major factor, in the second –aerosol effects are assumed to be the dominating. The results of the present study show that these two hypotheses do not contradict each other. Moreover, one can assume a synergetic effect of these two factors. High vertical velocity leads to the high supersaturation and to nucleation of small aerosols aloft needed for creation of supercooled droplets. At the same time, in-cloud nucleation increases vertical velocity, supposedly due to extra latent heat release by droplet diffusion growth and riming. We would like to stress, however, that charge separation is a result of the microphysical processes inside clouds (e.g. graupel-ice crystal collisions). Storm electrification is not directly caused by geographic location itself. Vertical velocity, wind shear and other dynamical factors themselves cannot lead to lightning. The role of the dynamical factors is to create favorable conditions for intensification of the microphysical processes of charge separation. Such considerations motivate efforts, as with the present study, to advance understanding of the fundamental mixed-phase microphysics in deep convective cells, if the diverse reasons for storm electrification are to be elucidated by the scientific community.

The effect of increase in the CCN concentration on cloud dynamics and microphysics is usually investigated by corresponding increase in parameter N_o in (1). Possible effects of slope parameter are often neglected. In these studies, a significant increase in supercooled CWC and supercooled droplet number concentrations at upper levels was reported. These changes in cloud microphysics were accompanied by the increase in the vertical updrafts (convective invigoration). The present study shows that the smallest CCN can play an important role also for clouds developing in a very polluted atmosphere (when N_o is high). Supersaturation in polluted clouds is

much lower than in clouds developing in clean air. At the same time at cold temperatures the concentration of droplets decreases (due to more riming). This may lead to an increase in supersaturation by up to several percent and to in-cloud nucleation. According to results obtained in this study, at the same value of N_o (if it is high), the concentration of ice crystals in cloud anvils can vary from several tens to several hundred per cm^3 depending on concentration of small CCN at cloud base. Assuming that small CCN exist in the CCN spectra, we found concentrations of ice crystals in cloud anvils of $350\ cm^3$, due to homogeneous freezing of the numerous supercooled droplets at about 10 km altitude, in agreement with the results of Heymsfield *et al.* (2009). Note that the increase in N_o without changing of the slope parameter also leads to increase in the concentration of the smallest CCN. Thus, in studies where only N_o was increased, an increase in the concentration of small CCN was guaranteed. For instance, substantial masses of supercooled water were measured by Rosenfeld and Woodley (2000) at a temperature $-37.5^\circ C$ in Texas summertime clouds. These cloud droplets gave rise to formation of about $500\ cm^{-3}$ ice crystals in cloud anvils due to homogeneous freezing. Such concentrations of supercooled droplets and ice crystals were simulated by Khain et al (2001) using an earlier version of the HUCM. The numerical results were interpreted in a sense that droplets in polluted continental clouds remain small and do not collide with ice particles during their ascent from cloud base till the homogeneous freezing level. Now we suppose that in-cloud nucleation played, possibly, an important role in the case of Texas clouds as well.

The in-cloud nucleation may be responsible for the well known experimental fact that DSDs at most vertical levels reveal the existence of very small droplets with diameters below $10\ \mu m$. Because the updraft speed tends to increase with height, the supersaturation increases continuously with height over a deep layer so that in-cloud droplet activation can occur over a deep layer. Thus, one expects the presence of very small droplets in the DSD over much of the cloudy updraft, even though each small droplet becomes larger than $10\ \mu m$ quickly by condensation, if they are continuously generated during ascent.

It is also shown that small aerosols allowing nucleation of droplets a few km above cloud base boost the speed of the cloudy updraft and lead to precipitation enhancement of maritime clouds.

A novel and striking conclusion of the present study is that the smallest aerosols have an important role in microphysics of maritime clouds. This imposes heavy demands on the

measurements of aerosols in the maritime atmosphere. The range of supersaturation variation in the laboratory should be increased to measure concentration of particles that can be activated at supersaturations as high as 10 % and even higher. The vertical variation of the droplet concentration throughout the depth of the troposphere must also be measured.

Often in the literature, the term “CCN” is defined as the sub-set of soluble aerosols (‘condensation nuclei [CN]’) that activate at supersaturations found in natural clouds (as reviewed by Rogers and Yau 1989). Observers of “CCN” tend to define them by assuming some fixed value of the maximum in-cloud supersaturation (e.g. 0.2% or 1%). While such definitions of “CCN” are practical, our work shows that the maximum in-cloud supersaturation can reach very high values, depending on the cloud-microphysical and dynamical conditions, so that such definitions only apply to some subset of natural clouds and not to all. In convective cloud ensembles, there is a broad, continuous probability distribution of vertical velocity among clouds (e.g. Phillips and Donner 2006) and hence also, of maximum in-cloud supersaturation. Thus, the choice of such a definition of “CCN” is quite subjective, as there is no sharp and universal distinction in nature between aerosols that activate in clouds and those that do not.

One can assume two main sources of the small CCN over the ocean. One source is related to chemical reactions involving trace gases condensing to form “secondary” ultrafine particles (the “Aitkin” mode), which then may later grow by more condensation or by collisions between APs to create the accumulation mode. Clarke and Kapustin (2002) analyzed aerosol observations from field campaigns over the Pacific Ocean and reported the existence of ultrafine aerosols with sizes smaller than $0.01 \mu\text{m}$ in the upper troposphere, especially near the outflow from deep convection (e.g. near the ITCZ). They assumed that these small APs, apparently generated in the outflow aloft, would be expected to subside through the free troposphere and may be eventually entrained into the boundary layer and into deep clouds through their lateral boundaries. The important role of such entrainment was stressed by Fridlind et al. (2004) and Phillips et al. (2005). Such secondary sources of ultrafine aerosols have been observed in the marine boundary layer too (e.g. Covert *et al.* 1992)

We also hypothesize that small aerosols can be of continental nature and penetrate the ocean with the intrusion of African dust creating favorable conditions for lightning in the ITCZ near the African coast (Chronis et al 2007). Since CCN represents only soluble fraction of AP, dust particles which are not small can activate just like small CCN. Observations of Saharan dust’s

composition over the Eastern Atlantic by Twohey *et al.* (2009) confirm that dust's slightly hygroscopic nature means that it can activate as a CCN, with a fraction of the dust size distribution activated at cloud-base. To answer the question as regards the nature and amount of small aerosols in the maritime tropical atmosphere more microphysical measurements of deep marine clouds and aerosol spectra in the zones of lightning over the ocean are required. The existence of the bimodal cloud droplet spectra in zones of high updrafts in cloud cores would be consistent with the existence of small aerosols.

If the role of small aerosols is as important as this study suggests, many concepts concerning the role of sea spray, giant CCN, etc. can be reconsidered, at least far as the microphysics of deep convective clouds developing over the oceans is concerned.

Note in conclusion that the effects from in-cloud nucleation of droplets discussed in the present study could not be found in many numerical models with bulk microphysics because they perform nucleation at cloud base only. We suppose that description of in-cloud nucleation has to be included in meteorological models (for instance, as done in the double-moment bulk scheme by Phillips *et al.* 2007a, 2009) for better understanding of aerosol effects. Moreover, the conclusions reached regarding the aerosol effects on precipitation should possibly be revised to take into account the role of smallest aerosols.

Acknowledgements. The authors express deep gratitude to Prof. Hudson and to Prof. Hobbs (Prof. Hobbs passed away in mid 2005) for useful discussions. The study has been performed under the support of the Israel Academy of Science (grant 140/07) and the Department of Homeland security of US (project HAMP). The second author was supported by the Office of Science (BER), US Department of Energy, with an award (grant number DE-SC0002383) for study of mechanisms for the influence from aerosols on glaciated clouds.

References

- Abdul-Razzak H. , S. J. Ghan, and C. Rivera-Carpio, 1998: A parameterization of aerosol activation. 1. Single aerosol type. *J. Geophys. Res.* 103, D6, 6123-6131.
- Baker, M. B., Jayaratne, E. R., Latham J., and C. P. R. Saunders, 1987: the influence of diffusional growth rates on the charge transfer accompanying rebounding collisions between ice crystals and soft hailstones. *Q. J. R. Meteorol. Soc.*, **113**, 1193–1215
- Black R. A. and Hallett J., 1999: Electrification of the hurricane, *J. Atmos. Sci*, 56, 2004-2028

- Black , M.L , R. W. Burpee, and F.D. Marks, Jr.1996: Vertical motion characteristics of tropical cyclones determined with airborne Doppler radar velocities. *J. Atmos. Sci.* **53**, 1887-1909.
- Blyth, A. M., J. Zhou, and J. Latham, 1998: Influence of ultra-giant nuclei on cumulus clouds observed during the Small Cumulus Microphysics Study in Florida. *AMS Conference on Cloud Physics 17-21 August, Everett, Washington* , 492-493.
- Bott A., 1989: A positive definite advection scheme obtained by nonlinear renormalization of the advective fluxes. *Mon. Wea. Rev.*, 117, 1006-1015.
- Bott, A., 1998: A flux method for the numerical solution of the stochastic collection equation *J. Atmos. Sci.*, 55, 2284-2293.
- Cecil D.J., E.J. Zipser, and S.W. Nebitt 2002a: Reflectivity, ice scattering, and lightning characteristics of hurricane eyewalls and rainbands. Part 1: Quantitative description. *Mon Wea. Rev.* 130, 769-784.
- Cecil D.J., E.J. Zipser, and S.W. Nebitt, 2002b: Reflectivity, ice scattering, and lightning characteristics of hurricane eyewalls and rainbands. Part 2: Intercomparison of observations. *Mon Wea. Rev.*, **130**, 785-801
- Christian, H. J., R. J. Blakeslee, D. J. Boccippio, W. L. Boeck, D. E. Buechler, Kevin T. Driscoll, S.J. Goodman, John M. Hall, W. J. Koshak, D. M. Mach, M. F. Stewart 2003: Global frequency and distribution of lightning as observed from space by the Optical Transient Detector, *J. Geophys. Res.*, 108(D1), 4005, doi:10.1029/2002JD002347.
- Christian, H. J., and J. Latham, 1998: Satellite measurements of global lightning. *Q. J. R. Meteorol. Soc.*, **124**, 1771-1773
- Chronis T, E. Williams, E. Anagnostou, and W. Petersen, 2007: African Lightning: indicator of tropical Atlantic cyclone formation. *EOS*, **88**, 40, 2 October 2007.
- Clarke, A. D. and V. Kapustin, 2002: A Pacific aerosol survey. Part I: A decade of data on particle production, transport, evolution, and mixing in the troposphere. *J. Atmos. Sci.*, 59, 363-382.
- Cohard, J-M., J-P. Pinty and C. Bedos, 1998: Extending Twomey's analytical estimate of nucleated cloud droplet concentrations from CCN spectra. *J. Atmos. Sci.*, 55, 3348-3357.
- Covert, D. S., V. N. Kapustin, P. K. Quinn, and T. S. Bates, 1992: New Particle Formation in the Marine Boundary Layer, *J. Geophys. Res.*, **97**(D18), 20581–20589

- Demetriades N.W.S and R.L Holle, 2006: Long-range lightning nowcasting applications for tropical cyclones. *Preprints, Conf. Meteorology Application of Lightning Data, Atlanta, AMS*, 9 pp.
- Dinger, J.E., H.B. Howell, and T.A. Wojciechowski, 1970: On the source and composition of cloud nuclei in a subsident air mass over the North Atlantic, *J. Atmos. Sci.*, 27, 791–797.
- Emde, K. and U. Wacker, 1993: Comments on the relationship between aerosol spectra, equilibrium drop size spectra, and CCN spectra. *Beitr. Phys. Atmosph.*, 66, 1-2, 157-162.
- Ferrier, B.S. and R.A. Houze 1989: One-dimensional time dependent modeling of GATE cumulonimbus convection. *J. Atmos. Sci.*, 46, 330-352.
- Fierro, A. O., J. M. Simpson, M. A. LeMone, J. M. Straka, and B. F. Smull, 2009: On how hot towers fuel the Hadley cell: An observational and modeling study of line-organized convection in the equatorial trough from TOGA COARE. *J. Atmos. Sci.*, 66:2730–2746
- Freud, E., D. Rosenfeld, M. O. Andreae, A. A. Costa, and P. Artaxo, 2008: Robust relations between CCN and the vertical evolution of cloud drop size distribution in deep convective clouds. *Atmos. Chem. Phys.*, 8, 1661–1675, 2008.
- Hallett, J. and Mossop, S. C., Production of secondary ice crystals during the riming process. *Nature*, 249, 26-28, 1974.
- Hegg, D. A., R. J. Ferek and P. V. Hobbs 1993: "Cloud Condensation Nuclei Over the Arctic Ocean in Early Spring" *J. Appl. Meteor.*, 34, 2076-2082.
- Helsdon, J. H., Wojcik, W. A., and R. D. Farley, 2001: An examination of thunderstormcharging mechanisms using a two-dimensional storm electrification model. *J. Geophys. Res*, 106, 1165-1192
- Helsdon, J. H., Gattaleeradapan, S., Farley, R. D., and C. Waits, 2002: An examination of the convective charging hypothesis: Charge structure, electric fields, and Maxwell currents. *J. Geophys. Res.*, 107, D22, 4630, doi:10.1029/2001JD001495
- Heymsfield A. J., A. Bansemer, G. Heymsfield and A.O. Fierro, 2009: Microphysics of maritime tropical convective updrafts at temperatures from -20°C to -60°C . *J. Atmos. Sci.*, 66, 3530-3565.
- Hobbs, P. V., 1971: Simultaneous airborne measurements of cloud condensation nuclei and sodium-containing particles over the ocean, *Quart. J. Roy. Meteor. Soc.*, 97, 263-271.
- Hobbs P.V. 1993: *Aerosol-cloud-climate interactions*. Academic Press, 236 pp.

- Hudson, J. G., (1984), Cloud Condensation Nuclei measurements within clouds, *J. Clim. and Appl. Meteorol* 23, 42-51
- Hudson J.G., and P.R. Frisbie 1991: Cloud condensation nuclei near marine stratus. *J. Geophys. Res.*, 96, 20795-20808.
- Hudson J.G., and H. Li, 1995: Microphysical contrasts in Atlantic stratus. *J. Atmos. Sci.*, 52, 3031-3040.
- Hudson, J. G., and S. S. Yum, 1997: Droplet spectral broadening in marine stratus, *J. Atmos. Sci.*, 54, 2642-2654.
- Hudson, J.G., and S.S. Yum, 2002: Cloud condensation nuclei spectra and polluted and clean clouds over the Indian Ocean. *J. Geophys.Res.*,107(D19),8022, doi:10.1029/2001JD000829.
- Jaenicke 1993: "Tropospheric Aerosols", Chapter in book by Aerosol-cloud-climate interactions edited by P. Hobbs. Academic Press, 236 pp.
- Jayarathne, R., Saunders, C. P. R., and J. Hallett, 1983: Laboratory studies of the charging of soft hail during ice crystal interactions. *Q. J. R. Meteorol. Soc.*, **103**, 609–630.
- Jiusto, J. E., Lala, G. G., 1981: CCN-supersaturation spectra slopes (k).*J. Rech. Atmos.*,**15**, 303–311.
- Jordan, C.L., Mean soundings for the West Indies area. *J. Meteor.*, 15, 91-97, 1958.
- Jorgensen, D. P., E.J. Zipser, and. M.A. LeMone, 1985: Vertical motions in intense hurricanes. *J. Atmos. Sci.*, 42, 839-856.
- Jorgensen, D.P., and M.A. LeMone 1989: Vertical velocity characteristics of oceanic convection. *J. Atmos. Sci.*, **46**, 621-640.
- Khain, A. P., and I. Sednev, 1996: Simulation of precipitation formation in the Eastern Mediterranean coastal zone using a spectral microphysics cloud ensemble model. *Atmos. Res.*, **43**, 77-110
- Khain, A. P., M. Ovtchinnikov, M. Pinsky, A. Pokrovsky, and H. Krugliak, 2000: Notes on the state-of-the-art numerical modeling of cloud microphysics. *Atmos. Res.* 55, 159-224.
- Khain A.P., Pinsky, M.B., M. Shapiro and A. Pokrovsky, 2001a: Graupel-drop collision efficiencies. *J. Atmos. Sci.*, **58**, 2571-2595.
- Khain A. P., D. Rosenfeld and A. Pokrovsky, 2001b: Simulation of deep convective clouds with sustained supercooled liquid water down to –37.5 C using a spectral microphysics model. *Geophysical Research Letters*, 28, 3887-3890.

- Khain A., A. Pokrovsky and M. Pinsky, A. Seifert, and V. Phillips, 2004: Effects of atmospheric aerosols on deep convective clouds as seen from simulations using a spectral microphysics mixed-phase cumulus cloud model Part 1: Model description. *J. Atmos. Sci.* 61, 2963-2982.
- Khain, A. D. Rosenfeld and A. Pokrovsky 2005: Aerosol impact on the dynamics and microphysics of convective clouds. *Quart. J. Roy. Meteor. Soc.* 131, 2639-2663.
- Khain, A. P., N. Benmoshe, A. Pokrovsky, 2008a Factors determining the impact of aerosols on surface precipitation from clouds: an attempt of classification. *J. Atmos. Sci.* 65, 1721-1748.
- Khain, A. N. Cohen, B. Lynn and A. Pokrovsky, 2008b: Possible aerosol effects on lightning activity and structure of hurricanes. *J. Atmos. Sci.* 65, 3652-3667.
- Khain, A. P. 2009. Effects of aerosols on precipitation: a review. *Environ. Res. Lett.* 4 015004.
- Khain, A. P., B. Lynn and J. Dudhia, 2010a: Aerosol effects on intensity of landfalling hurricanes as seen from simulations with WRF model with spectral bin microphysics, *J. Atmos. Sci.* 67, 365-384.
- Khain, A., A. Pokrovsky, D. Rosenfeld , U. Blahak and A. Ryzhkov, 2010b: The role of CCN in precipitation and hail in a mid-latitude storm as seen in simulations using a spectral (bin) microphysics model in a 2D dynamic frame. *Atmos. Res.* (in press).
- Khain, A., M. Pinsky, N. Benmoshe, and A. Pokrovsky 2010c: Turbulent effects on cloud microstructure and precipitation of deep convective clouds as seen from simulations with a 2-D spectral microphysics cloud model, *J. Atmos. Sci.* (*in revision*)
- Korolev, A. V., 1994: A study of bimodal droplet size distributions in stratiform clouds. *Atmos. Res.* , 32, 143-170.
- Korolev A., and I. Mazin, 2003: Supersaturation of water vapor in clouds. *J. Atmos. Sci.*, 60, 2957-2974.
- Korolev A., 2007: Limitations of the Wegener–Bergeron–Findeisen Mechanism in the Evolution of Mixed-Phase Clouds. *J. Atmos. Sci.*, 64, 3372-3375
- Latham, J., and J. E. Dye, 1989: Calculations on the electrical development of a small thunderstorm. *J. Geophys. Res.*, **94**, D12, 13141-13144
- Levin Z., and W.R. Cotton (Eds.), 2009: Aerosol pollution impact on precipitation: A Scientific Review, Springer. 386 pp.
- Ludlam F .H.(1980), *Clouds and Storms*. The Pensilavnia State University Press, 405 pp.

- Martin G.M., D. W. Johnson and A. Spice, 1994: The measurements and parameterization of effective radius of droplets in warm stratocumulus clouds. *J. Atmos. Sci.*, **51**, 1823-1842.
- Meyers, M. P., DeMott, P., W. R. Cotton, 1992: Evaluation of the Potential for Wintertime Quantitative Precipitation Forecasting over Mountainous Terrain with an Explicit Cloud Model. Part I: Two-Dimensional Sensitivity Experiments. *J. Appl. Meteor.* **31**, 26–50.
- Michalon, N., Nassif, A., Saouri, T., Royer, J. F., and C. A. Pontikis, 1999: Contribution to the climatological study of lightning. *Geophys. Res. Lett.*, **26**(20), 3097-3100
- Molinie´, J., and C. A. Pontikis, 1995: A climatological study of tropical thunderstorm clouds and lightning frequencies on the French Guyana coast. *Geophys. Res. Lett.*, **22**, 1085-1088
- Molinari J., Moore P., and V. Idone, 1999: Convective structure of hurricanes as revealed by lightning locations, *Mon. Wea. Rev.*, **127**, 520-534
- Norville, K., Baker, M. B., and J. Latham, 1991: A numerical study of thunderstorm electrification: model development and case study. *J. Geophys. Res.*, **96**, D4, 7463–7481
- Ochs, H.T., 1978: Moment-Conserving Techniques for Warm Cloud Microphysical Computation. Part II. Model Testing and Results. *J. Atmos. Sci.*, **35**, 1959–1973.
- Orville, R. E., and R. W. Henderson, 1986: Global distribution of midnight lightning: September 1977 to August 1978. *Mon. Wea. Rev.*, **114**, 2640-2653
- Ovtchinnikov, M; Kogan, YL; Blyth, AM (2000) An investigation of ice production mechanisms in small cumuli using a 3-D cloud model with explicit microphysics. Part II: Case study of New Mexico cumulus clouds, *Journal of the Atmospheric Sciences*, **57**(18), pp3004-3020.
- Petersen W. A., R. C. Cifelli, S. A. Rutledge, B. S. Ferrier and B. F. Smull, 1999: Shipborne Dual-Doppler Operations during TOGA COARE: Integrated Observations of Storm Kinematics and Electrification Bulletin of the American Meteorological Society Vol. 80, No. 1, January 1999, 81-97.
- Phillips, V. T. J., Blyth, A. M., Choullarton, T. W., Brown, P. R. A., and J. Latham, 2001: The glaciation of a cumulus cloud over New Mexico. *Q. J. R. Meteorol. Soc.*, **127**, 1513-1534
- Phillips, V. T. J., Choullarton, T. W., Blyth, A. M., and J. Latham, 2002: The influence of aerosol concentrations on the glaciation and precipitation production of a cumulus cloud. *Q. J. R. Meteorol. Soc.*, **128**, 951-971

- Phillips, V. T. J., Choulaton, T. W., Illingworth, A. J., Hogan, R. J., and P. R. Field, 2003: Simulations of the glaciation of a frontal mixed-phase cloud with the Explicit Microphysics Model (EMM). *Q. J. R. Meteorol. Soc.*, 129, 1351-1371
- Phillips, V. T. J., Sherwood, S. C., Andronache, C., Bansemer, A., Conant, W. C., DeMott, P. J., Flagan, R. C., Heymsfield, A., Jonsson, H., Poellot, M., Rissman, T. A., Seinfeld, J. H., Vanreken, T., Varutbangkul, V., and J. C. Wilson, 2005: Anvil glaciation in a deep cumulus updraft over Florida simulated with an Explicit Microphysics Model. I: The impact of various nucleation processes. *Q. J. R. Meteorol. Soc.*, 131, 2019-2046
- Phillips, V. T. J., and L. J. Donner, 2006: Cloud microphysics, radiation and vertical velocities in two- and three-dimensional simulations of deep convection. *Q. J. R. Meteorol. Soc.*, 132, 3011-3033
- Phillips, V. T. J., Donner, L. J., and S. Garner, 2007a: Nucleation processes in deep convection simulated by a cloud-system resolving model with double-moment bulk microphysics. *J. Atmos. Sci.*, 64, 738-761
- Phillips V., A. Khain, and A. Pokrovsky 2007b: The Influence of Melting on the Dynamics and Precipitation Production in Maritime and Continental Storm-Clouds. *J. Atmos. Sci.*, 64, no. 2, 338-359
- Pinsky, M., A. P. Khain, and M. Shapiro 2001: Collision efficiency of drops in a wide range of Reynolds numbers: Effects of pressure on spectrum evolution. *J. Atmos. Sci.* 58, 742-764.
- Pinsky, M. and A. P. Khain, 2002: Effects of in-cloud nucleation and turbulence on droplet spectrum formation in cumulus clouds. *Quart. J. Roy. Meteorol. Soc.*, 128, 1-33.
- Pinsky M., A. Khain and H. Krugliak, 2008: Collisions of cloud droplets in a turbulent flow. Part 5: Application of detailed tables of turbulent collision rate enhancement to simulation of droplet spectra evolution. *J. Atmos. Sci.* , 63, 357-374
- Pruppacher, H. R., A new look at homogeneous ice nucleation in supercooled water drops. *J. Atmos. Sci.*, 52, 1924-1933, 1995.
- Pruppacher, H. R., and J. D. Klett, 1997: *Microphysics of clouds and precipitation*. 2-nd edition, Oxford Press, 1997, 963p.
- Radke, L.F., and P.V. Hobbs, An automatic cloud condensation nuclei counter, *J. Appl. Meteor.*, 8, 105-109, 1969.

- Radke, L.F., and P.V. Hobbs, 1976: Cloud condensation nuclei on the Atlantic seaboard of the United States, *Science*, 193, 999–1002.
- Rogers R. R. and Yau M. K, 1989: A Short Course in Cloud Physics, Pergamon press. 293pp.
- Rosenfeld, D., and I. M. Lensky, 1998: Satellite-based insights into precipitation formation processes in continental and maritime convective clouds. *Bull. Am. Meteorol. Soc.*, **79**, 2457–2476.
- Rosenfeld D, R. Lahav, A. Khain, and M. Pinsky, 2002: The role of sea spray in cleaning air pollution over ocean via cloud processes. *Science* 297, 1667-1670.
- Saunders, C.P.R. (1993). A review of thunderstorm electrification processes, *J. Appl. Meteor.*, 32, 642-655.
- Saunders, C. P. R., Keith, D., and R. P. Mitzeva, 1991: The effect of liquid water on thunderstorm charging. *J. Geophys. Res.*, **96**, 11007-11017
- Segal, Y., A. Khain, and M. Pinsky, 2003: Thermodynamic factors influencing the bimodal spectra formation in cumulus clouds. *Atmos. Res.* 66, 43-64.
- Segal, Y., and A. Khain, 2006: Dependence of droplet concentration on aerosol conditions in different cloud types: application to droplet concentration parameterization of aerosol conditions, *J. Geophys. Res.* Vol. 111, D15204, doi:10.1029/2005JD006561.
- Shao X.M., Harlin J., Stock M., Stanley M., Regan A., Wiens K., Hamlin T., Pongratz M., Suszcynsky D. and Light T., Los Alamos National Laboratory, Los Alamos, N.M, 18 October 2005, Katrina and Rita were lit up with lightning, *EOS*, Vol. 86, No.42, page 398-399.
- Sherwood S.C., V. Phillips and J. S. Wettlaufer (2006). Small ice crystals and the climatology of lightning. *Geophys. Res. Letters*, 33, L058804, doi. 10.1029/2005GL.
- Song, N., and J. Marwitz, 1989: A numerical study of the warm rain process in orographic clouds. *J. Atmos. Sci.*, **46**, 3479–3486
- Szoke, E.J., E.J. Zipser, and D.P. Jorgensen, 1986: A radar study of convective cells in mesoscale systems in GATE. Part 1: Vertical profile statistics and comparison with hurricanes. *J. Atmos. Sci.*, 43, 182-197.
- Tao W-K., X. Li, A. Khain, T. Matsui, S. Lang, and J. Simpson· The role of atmospheric aerosol concentration on deep convective precipitation: Cloud-resolving model simulations. *J. Geophys. Res.* VOL. 112, D24S18, doi:10.1029/2007JD008728, 2007

- Takahashi, T., 1978: Riming electrification as a charge generation mechanism in thunderstorms. *J. Atmos. Sci.*, 35, 1536-1548.
- Takahashi, T., 1984: Thunderstorm electrification – A numerical study. *J. Atmos. Sci.*, **41**, 2541–2558
- Takahashi, T., Endoh, T., and G. Wakahama, 1991: Vapor diffusional growth of free-falling snow crystals between –3 and –23 C. *J. Meteor. Soc. Japan*, 69, 15-30.
- Takahashi T., and K. Kuhara, 1993: Precipitation mechanisms of cumulonimbus clouds at Pohnpei, Micronesia. *J. Meteor. Soc. Japan*, 71, 21-31
- Twohy, C. H., et al. (2009), Saharan dust particles nucleate droplets in eastern Atlantic clouds, *Geophys. Res. Lett.*, 36, L01807, doi:10.1029/2008GL035846.
- Twomey, S., 1959: The nuclei of natural cloud formation: the supersaturation in natural clouds and the variation of cloud droplet concentration. *Geofis. Pura et Appl.*, 43, 243-249.
- Twomey, S., 1968: On the composition of cloud nuclei in the northeastern United States, *J. de Rech. Atmos.*, 3, 281-285.
- Twomey, S., 1971: The composition of cloud nuclei, *J. Atmos. Sci.*: 28, 377–381.
- Twomey S. and T.A. Wojciechowski, 1969: Observations of the geographical variation of cloud nuclei. *J. Atmos. Sci.*, 26, 648-651.
- Vali, G., Freezing rate due to heterogeneous nucleation. *J. Atmos. Sci.*, 51, 1843-1856, 1994.
- Van den Heever, S. C.; G.G. Carrió, .; W.R. Cotton, .; P. J. Demott, . A. J Prenni, 2006: Impacts of Nucleating Aerosol on Florida Storms. Part I: Mesoscale Simulations. *J. Atmos. Sci.*, 63, 7, pp.1752-1775
- Wang C. 2005: A modelling study of the response of tropical deep convection to the increase of cloud condensational nuclei concentration: 1. Dynamics and microphysics. *J. Geophys. Res.*, v. 110; D21211, doi:10.1029/2004JD005720.
- Warner, J., 1969a: The microstructure of cumulus cloud. Part 1. General features of the droplet spectrum, *J. Atmos. Sci.*, 26, 1049-1059.
- Warner, J., 1969 b: The microstructure of cumulus cloud. Part 2. The effect of droplet size distribution of the cloud nucleus spectrum and updraft velocity. *J. Atmos. Sci.*, 26, 1272-1282.
- Warner, J., 1973: The microstructure of cumulus cloud: Part 4: The effect on the droplet spectrum of mixing between cloud and environment. *J. Atmos. Sci.*, **30**, pp. 256-261.

- Williams, E., Rosenfeld, D., Madden, N., Labrada, C., Gerlach, J., and L. Atkinson, 1999: The role of boundary layer aerosol in the vertical development of precipitation and electrification: Another look at the contrast between lightning over land and over ocean, Preprints, in *Eleventh International Conference on Atmospheric Electricity*, pp. 754 –757, Am. Meteorol. Soc., Boston, Mass.
- Williams, E., and co-authors 2002: Contrasting convective regimes over the Amazon: implications for cloud electrification. *J. Geophys. Res.*, **107**, D20, 8082, doi:10.1029/2001JD000380
- Williams E, G., Satori, 2004: Lightning, thermodynamic and hydrological comparison of the two tropical continental chimneys. *J. Atmos. And Solar-terrestrial Phys.* 66, 1213-1231.
- Williams E., T. Chan and D. Boccippio, 2004: Islands as miniature continents: Another look at the land-ocean lightning contrast. *J. Geophys. Res.*, v.109, D16206, doi:10.1029/2003JD003833
- Williams E., V. Mushtak, D. Rosenfeld, S. Goodman and D. Boccippio, 2005: Thermodynamic conditions favorable to superlative thunderstorm updraft, mixed phase microphysics and lightning flash rate. *Atmos. Res.*, 76, 288-306.
- Williams, E., and S. Stanfill, 2002: The physical origin of the land-ocean contrast in lightning activity. *Comptes Rendus Physique*, **3** (10), 1277-1292
- Willoughby, H.E., Jorgensen D.P., Black R.A., and Rosenthal S.L., 1985: Project STORMFURY, A Scientific Chronicle, 1962-1983, Bull. Amer. Meteor. Soc., 66, 505-514.
- Yin, Y., Z. Levin, T. Reisin, and S. Tzivion, 2000: The effects of giant cloud condensational nuclei on the development of precipitation in convective clouds: A numerical study. *Atmos. Res.*, 53, 91-116